FACILITY FORM 602

N64-27901
(ACCESSION NUMBER)

77
(PAGES)

CR-56277
(NASA CR OR TMX OR AD NUMBER)

(THRU)

1
(CODE)

29
(CATEGORY)

ORBITING SATELLITE SURFACE TEMPERATURE PREDICTION AND ANALYSIS

FINAL REPORT

4 February 1963 - 3 February 1964

Contract No. NAS9-1059

MRI Project No. 2669-E

OTS PRICE

XEROX $ 7.60

MICROFILM $ _____

NASA - Manned Spacecraft Center
Houston, Texas 77001

MIDWEST RESEARCH INSTITUTE

A PROGRAM TO DETERMINE SPACECRAFT HEAT LOADS AND TEMPERATURES....

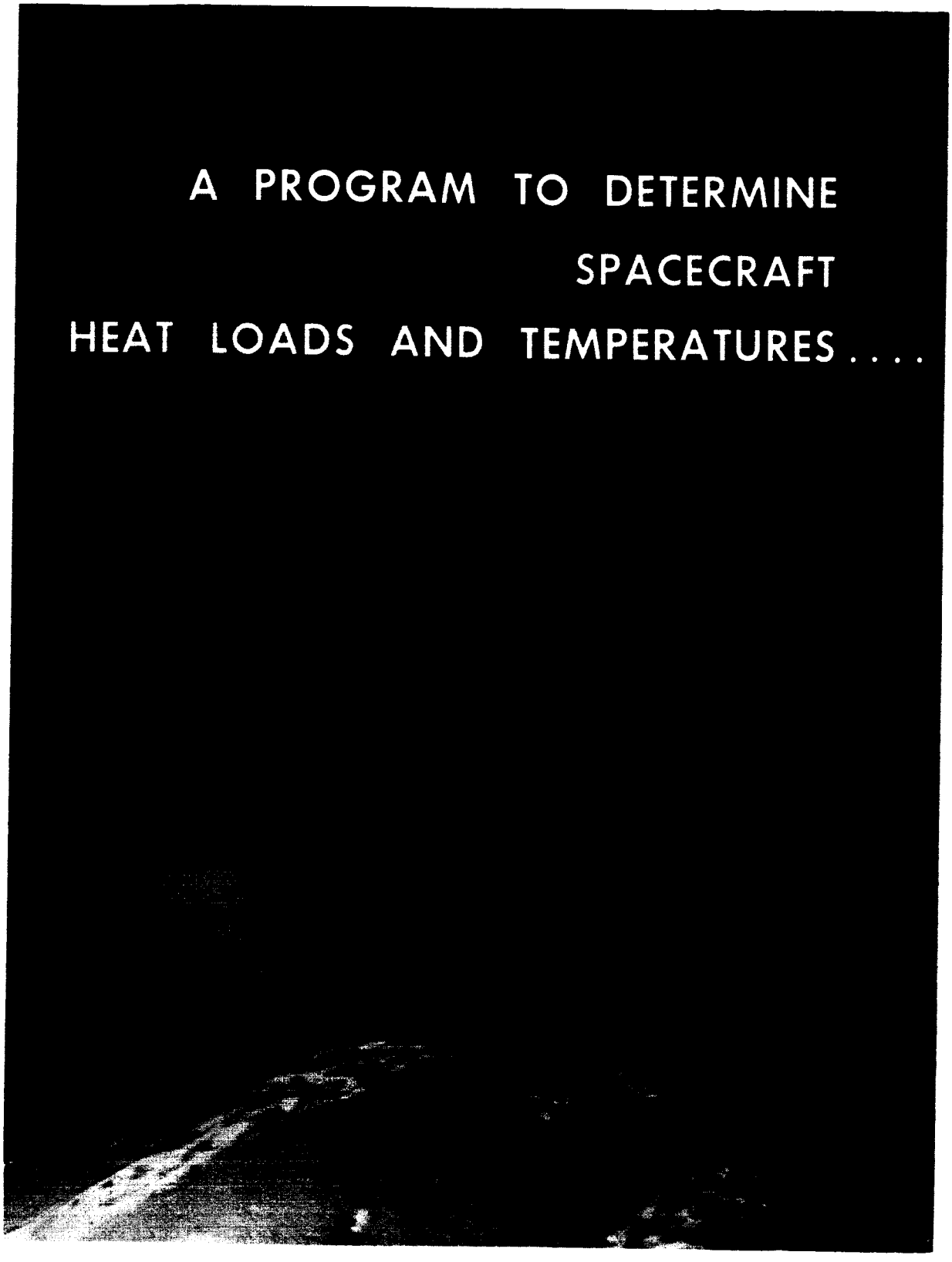

MIDWEST RESEARCH INSTITUTE

ORBITING SATELLITE SURFACE TEMPERATURE PREDICTION AND ANALYSIS

by

Harold L. Finch
Duncan Sommerville
Roger Schroeder
Dean Lawrence

FINAL REPORT
4 February 1963 - 3 February 1964

Contract No. NAS9-1059

MRI Project No. 2669-E

For

NASA - Manned Spacecraft Center
Houston, Texas 77001

PREFACE

This final report covers the activities conducted during the 12-month contract period from 4 February 1963 to 4 February 1964, on the project entitled "Orbiting Satellite Surface Temperature Prediction and Analysis." The work was authorized January 31, 1963, by the NASA Manned Spacecraft Center under Contract No. NAS9-1059, and was performed by Midwest Research Institute, Kansas City, Missouri, under Project No. 2669-E.

Mr. Harold L. Finch, Project Leader, developed the theory and worked on all phases of the program. Mr. Duncan Sommerville supervised the programming.

Mr. Roger Schroeder contributed to the selection of an applicable set of reference coordinate systems. Mr. Dean Lawrence performed the numerical analysis. Others who made significant technical contributions were Dr. Harry Sauer, Mr. Gary Sears, and Miss Rosemary Moran.

Mr. Robert McGuire made the technical illustrations accompanying this report.

Approved for:

MIDWEST RESEARCH INSTITUTE

Harold L. Stout

Harold L. Stout, Director
Engineering Division

26 February 1964

lw

TABLE OF CONTENTS

	Page No.
Summary	1
List of Symbols	3
I. Introduction	6
II. Celestial Mechanics Theory: Coordinate Systems	8
A. Vehicle Coordinates	9
B. Planet Coordinates	11
C. Celestial Coordinates	12
D. The Sun's Position	17
III. Heat Transfer Theory	24
A. Heat Loads	24
B. Transient Temperatures	29
IV. Numerical Analysis	33
A. Method of Integration	33
B. Step-Size and Error Analysis	33
C. Integration Technique When Function is Nondifferentiable	35
V. Digital Computer Program	36
A. Summary of Program Capabilities and Applications	36
B. Assumptions	38
VI. Typical Test Cases	40
A. Lunar Excursion Module Hypothetical Mission	40
B. Vanguard and Explorer Earth Satellites	42
VII. Conclusions and Recommendations	45
References	46
Appendix A - Intersection of Orbit and Shadow	47
Appendix B - Radiation Heat Transfer Derivations	51
Appendix C - Discussion of Practical Integration Step-Size	69

TABLE OF CONTENTS (Concluded)

List of Illustrations

Fig. No.	Title	Page No.
1	Vehicle Coordinate System for a Typical Spacecraft . . .	10
2	Planet Coordinate Systems for Spinning and Oriented Vehicles	11
3	Relationship between Orbit and General Celestial Coordinate System	14
4	Celestial Coordinate System for Earth (Geocentric) and Other Planets (Modified Heliocentric)	16
5	Celestial Coordinate System for the Moon (Selenographic).	16
6	Sun's Position Relative to the Celestial Coordinate System	18
7	Sun's Position Relative to the Planet Coordinate System	18
8	Sun's Position Relative to the Vehicle Coordinate System (Planet-Oriented)	22
9	Sun's Position Relative to the Vehicle Coordinate System (Sun-Oriented)	22
10	Principal External Heat Loads	24
11	Angular Variables for Determining Configuration Factors of Oriented Vehicles	28
12	Simulated Lunar Excursion Module; Elements Face Away from the Moon	43
13	Simulated Lunar Excursion Module; Elements Face the Moon	44
A-1	Intersection of Planet's Shadow and Orbit Plane	48
B-1	Mathematical Model for Deriving General Thermal Radiation Equation	51
B-2	Seavey's Model for Determining Radiation between Two Spheres of Uniform Brightness.	54
B-3	Geometry for Determining Heat Exchange between Planet and Spinning Vehicle	58
B-4	Heat Emitted by an Element of a Variable Temperature Planet	58
B-5	Configuration Factors: Approximate and Numerical Solutions Compared	61
B-6	Geometry for Determining Heat between Planet and Vehicle Element	64
B-7	Angular Variables for Determining Configuration Factors of Oriented Vehicles	65

SUMMARY

A computer program to predict the thermal history of spacecraft in orbit has been developed by Midwest Research Institute for the National Aeronautics and Space Administration's Manned Spacecraft Center. The objective of the project was to develop an analytical tool to determine impinging radiation heat loads and/or transient temperatures of vehicles[a] orbiting the moon, earth, or any other planet, except Pluto.

One of the unique features of the program is the ability to compensate for surface temperature gradients of the celestial body being orbited, thereby making the program especially applicable to Project Apollo and other moon programs.

Spinning, planet-oriented, or sun-oriented vehicles can be evaluated. Up to 200 surface elements having various combinations of eight coatings and substrates can be analyzed in each case. Material thermophysical properties may be constant or temperature-dependent.

The primary consideration in selecting celestial coordinate systems for this program was that they should be compatible with available astronomical references so as to minimize input data compilation time and effort by the user. Methods for determining impinging heat loads and transient surface temperatures are based on fundamental heat transfer theory.

Numerical techniques for integrating the general thermal differential equation are optimized with respect to accuracy and computation time. A major contribution of the numerical analysis was the discovery and elimination of a significant error arising from the misapplication of integration techniques employed in some previous studies.

This initial project did not consider heat exchange between surface elements; however, the program can be expanded to be compatible with existing heat conduction programs. Programming has been done in FORTRAN to facilitate such modifications.

a/ The term "vehicle" is used to denote all manned and unmanned satellites, spacecraft, and other objects in orbit.

Hundreds of hypothetical test cases were run to check out specific routines and functions as well as to evaluate the over-all program. The Lunar Excursion Module moon voyage, being planned for the late 1960's, was simulated on the computer. The results confirmed the importance of the program's ability to account for the moon's surface temperature gradients. This feature eliminated large errors in determining lunar thermal emission and resulted in improved vehicle temperature predictions, in one case by ±100°R. Simulated runs gave time-temperature curves that closely approximated the actual curves of the Explorer and Vanguard satellites; for example, the equilibrium temperature of the latter was estimated to within 4°R of the measured value.

LIST OF SYMBOLS

A - Area

a - Semimajor axis of ellipse

b - Semiminor axis of ellipse

C_p - Specific heat

c - Distance between the center and focus of an ellipse

D - Distance between orbiting vehicle and center of planet

DEC - Declination (latitude of sun w.r.t. X_c, Y_c, Z_c axes)

E - Eccentric anomaly

E_n - Total error due to numerical integration

e - Eccentricity of ellipse

$e_{t,n}$ - One-step truncation error

$e_{t,a}$ - Accumulated truncation error over steps 1 to n-1

e_{ro} - Accumulated round-off error over n steps

F - Radiation configuration factor

G - Gravitational constant

H - Altitude

h - Thickness of vehicle skin

i - Inclination of orbit plane

M_p - Mass of planet

P - Period (time to complete one orbit)

Q_g - Internal heat generation

q - Heat flux

R - Reflectivity constant (albedo)

RA - Right ascension (longitude of sun w.r.t. X_c, Y_c, Z_c axes)

r_p - Radius of planet

S - Solar constant

T - Temperature

T_m - Minimum planet temperature (dark side of planet)

T_p - Average planet temperature

t - Time

V - Volume

X, Y, Z - Coordinate axes

α - Angle between planet-sun line and X_p axis

α_p - Absorptivity of vehicle material w.r.t. planet-emitted radiation

α_s - Absorptivity of vehicle material w.r.t. solar radiation

β - Angle between planet-sun line and Z_p axis

γ - Angle between planet-sun line and Y_p axis

δ - Angle between vehicle-sun line and vehicle-vehicle element line

ϵ - Angle between vehicle element-vehicle line and vehicle-planet line

ϵ_v - Emissivity of vehicle material

θ_s - Angle between sun-planet line and planet-vehicle line

Λ' - Angle between X_v axis and projection of vehicle-vehicle element line on X_v, Y_v plane

Λ_s - Angle between X_v axis and projection of sun-vehicle line on X_v, Y_v plane

ρ - Density

Σ - Angle between X_p axis and projection of sun-planet line on X_p, Y_p plane

σ - Stefan-Boltzmann constant

Υ - Vernal equinox (an intersection of earth's equator and the ecliptic)

ϕ - True anomaly

$\Delta\phi$ - Integration step-size as specified in input data. Program may choose to use a smaller increment.

ϕ_{in} - Value of ϕ where vehicle passes into the planet's shadow

ϕ_{out} - Value of ϕ where vehicle passes out of the planet's shadow

ϕ_c - Angle between vehicle-planet-sun plane and vehicle element-vehicle-planet plane

Ω - - Longitude of ascending node

Ω' - Angle between Z_v axis and vehicle-vehicle element line

Ω_s - Angle between Z_v axis and sun-vehicle line

$\underline{\Omega}$ - Autumnal equinox (an intersection of earth's equator and the ecliptic)

ω - Argument of perifocus

Subscripts

c - Celestial

e - Emitting body

o - Initial condition

p - Planet

r - Receiving body

s - Sun

v - Vehicle

I. INTRODUCTION

Thermal radiation and temperature play an important role in the development of spacecraft and their components. A computer program to predict these variables continuously as a vehicle[a] orbits a celestial body has been developed by Midwest Research Institute (MRI) for the National Aeronautics and Space Administration's Manned Spacecraft Center (NASA MSC). This program will assist thermal and structural engineers in analyzing actual and hypothetical spacecraft and missions.

A survey of the literature was conducted before initiating work on this project. The search revealed that existing methods were either too simplified, too specialized, or did not fulfill unique NASA MSC requirements.

One important criterion not included in previous approaches is the consideration of the effects of planet[b] surface temperature gradients on spacecraft heating. Surface temperature variations of cloud-covered planets are relatively small and unpredictable, thus their neglect in analyses of earth satellites is acceptable. On the other hand, temperature gradients on some planets are large and should not be neglected. The program developed under this contract is to be applicable to Project Apollo; therefore, it incorporates theory that accounts for the extreme surface temperature variations of the moon, as well as other nonuniformly radiating bodies.

While none of the available methods could be used "off the shelf," it was deemed that one of these, an Air Force computer program,[c] could be revised and expanded to fulfill NASA MSC requirements. MRI was contracted in February 1963 to develop the theory and to perform the necessary modifications to the existing Air Force program.

The over-all objective of the project was to develop an operable IBM 7094 FORTRAN program to determine impinging solar, planetary, and albedo[d]

---

a/ The term vehicle is used to denote all manned and unmanned satellites, spacecraft, and other objects in orbit.

b/ The term planet in this report refers to the celestial body being orbited, whether it be the moon, the earth, or another planet.

c/ The Air Force program[1] was directed by Mr. Harold L. Finch, who is now a staff member of Midwest Research Institute and is Project Leader of the program described in this report.

d/ Albedo is considered in this report to be solar heat that is reflected from a planet and its atmosphere.

heat fluxes and/or temperatures of spinning vehicles or of a large number of infinitesimal surface elements of a vehicle that is planet- or sun-oriented.[a] Internal conduction is neglected in this initial study. While the program is capable of analyzing orbits about all planets except Pluto,[b] special emphasis has been placed on problems associated with lunar missions.

The transition from the existing Air Force program to a program that meets the above objectives was accomplished by performing the following steps:

1. The existing program was checked out and inoperable routines were debugged on the 7094 computer.

2. The slow orbit-shadow intersection routine was replaced by an improved numerical method.

3. The program was reorganized into a pilot routine and a number of basic subroutines to facilitate debugging, recompiling, and program modifications.

4. A theory to account for planet surface temperature extremes was developed and programmed.

5. The program was expanded to include planet- and sun-oriented vehicles.

6. The program was written to analyze up to 200 specific points on oriented vehicles. The points are assumed to be thermally insulated from the surrounding surface.

7. The input routine was made to accept standard[c] NASA decks of temperature-dependent material properties.

8. The program was developed to analyze internal heat as a function of time. Up to 10 duty cycles per orbit are allowed. Different elements may have different internal heating cycles.

---

a/ An object is planet-oriented if the line connecting the vehicle and planet centers passes through the same vehicle surface element for all positions in the orbit path. Similarly an object is sun-oriented if the vehicle-sun line passes through the same surface element at all times.

b/ Pluto orbits could be analyzed if sufficient planetary data were available.

c/ Standard NASA deck refers to material decks using a format developed by the NASA MSC Thermal Analysis Section.

9. Standard data (e.g., astronomical planet data) were incorporated into the program body to facilitate preparation of input data.

10. The input routine was written so that parametric studies can be made with a minimum amount of data preparation in successive cases.

11. Output options of printing temperatures and/or impinging heats were provided.

12. Numerous minor improvements were incorporated into the program.

13. Check cases to test the program logic and theory were devised and run.

Sections II, III, and IV of this final report contain the fundamental celestial mechanics, heat transfer, and numerical analysis theories that are incorporated into the computer program. A description of the program and its use is given in Section V.

A hypothetical Lunar Excursion Module orbit and actual Explorer and Vanguard missions were run on the computer. The results of these cases are summarized and discussed in Section VI. Recommendations for further applications of the program are given in Section VII.

Complete derivations of equations used in Sections II and III are included in Appendices A and B. A discussion of practical numerical integration step-sizes is given in Appendix C.

A User's Manual giving a detailed description of the computer program and explanations of input data for sample cases supplements the final report.

II. CELESTIAL MECHANICS THEORY: COORDINATE SYSTEMS

Three questions must be considered before vehicle heat loads can be determined:

1. What is the location of each vehicle surface element being analyzed? This question is not applicable to spinning satellites.

2. Where is the vehicle with respect to the planet being orbited?

3. What is the celestial location of the vehicle?

The required answers can be obtained in terms of vehicle, planet, and celestial coordinates. These three systems are identified throughout the report by the following notation:

Vehicle coordinates - X_v, Y_v, Z_v

Planet coordinates - X_p, Y_p, Z_p

Celestial coordinates - X_c, Y_c, Z_c

These three coordinate systems are summarized in the table at the end of this section and are described in detail below.

A. Vehicle Coordinates

It is assumed that the period of rotation of a spinning vehicle is considerably less than that of individual heat fluxes; in other words, it is spinning fast enough that impinging thermal radiation is uniformly distributed over the vehicle surface. Consequently, no distinction between surface elements is required and X_v, Y_v, Z_v coordinates are not applicable.

On the other hand, the incident heat flux on an oriented vehicle can vary considerably from one surface position to another. For example, element No. 1 on the planet-oriented vehicle shown in Fig. 1a receives heat emitted by the planet while element No. 2 does not. Consequently, a system to answer the first question (what is the location of each element being analyzed?) is required for the thermal analysis of oriented spacecraft.

Vehicle coordinates that are meaningful to the program user will be illustrated for the vehicle in Fig. 1a. The complex configuration is first replaced with a spherical mathematical model as shown in Fig. 1b and surface elements, Nos. 1' and 2' on the sphere are selected so that they have the same space orientations as the corresponding vehicle elements, Nos. 1 and 2.

If the orbiting body is planet-oriented, surface positions on the sphere are defined with respect to the coordinate system illustrated in the schematic, Fig. 1c. The origin is at the sphere's center and the X_v axis is directed toward the planet's center of mass. The Z_v axis is normal to the orbit plane and the Y_v axis is at right angles to the X_v axis in the orbit plane in a direction such that X_v, Y_v and Z_v form a right-handed coordinate system. Surface elements are defined by the angles Λ' and Ω', as shown in Figs. 1c and 1d. The angle Λ' is measured from the X_v axis to the element's projection on the X_v, Y_v plane ($0° \leq \Lambda' < 360°$); Ω' is measured from the Z_v axis to the element ($0° \leq \Omega' \leq 180°$).

If the orbiting body is sun-oriented, surface points or features are located with respect to the system shown in Fig. 1d. The origin is again at the sphere's center, but the X_v axis is directed toward the sun. The Y_v axis is in the orbit plane and the Z_v axis completes the orthogonal system. Surface elements are described by the coordinates, Λ' and Ω' as before.

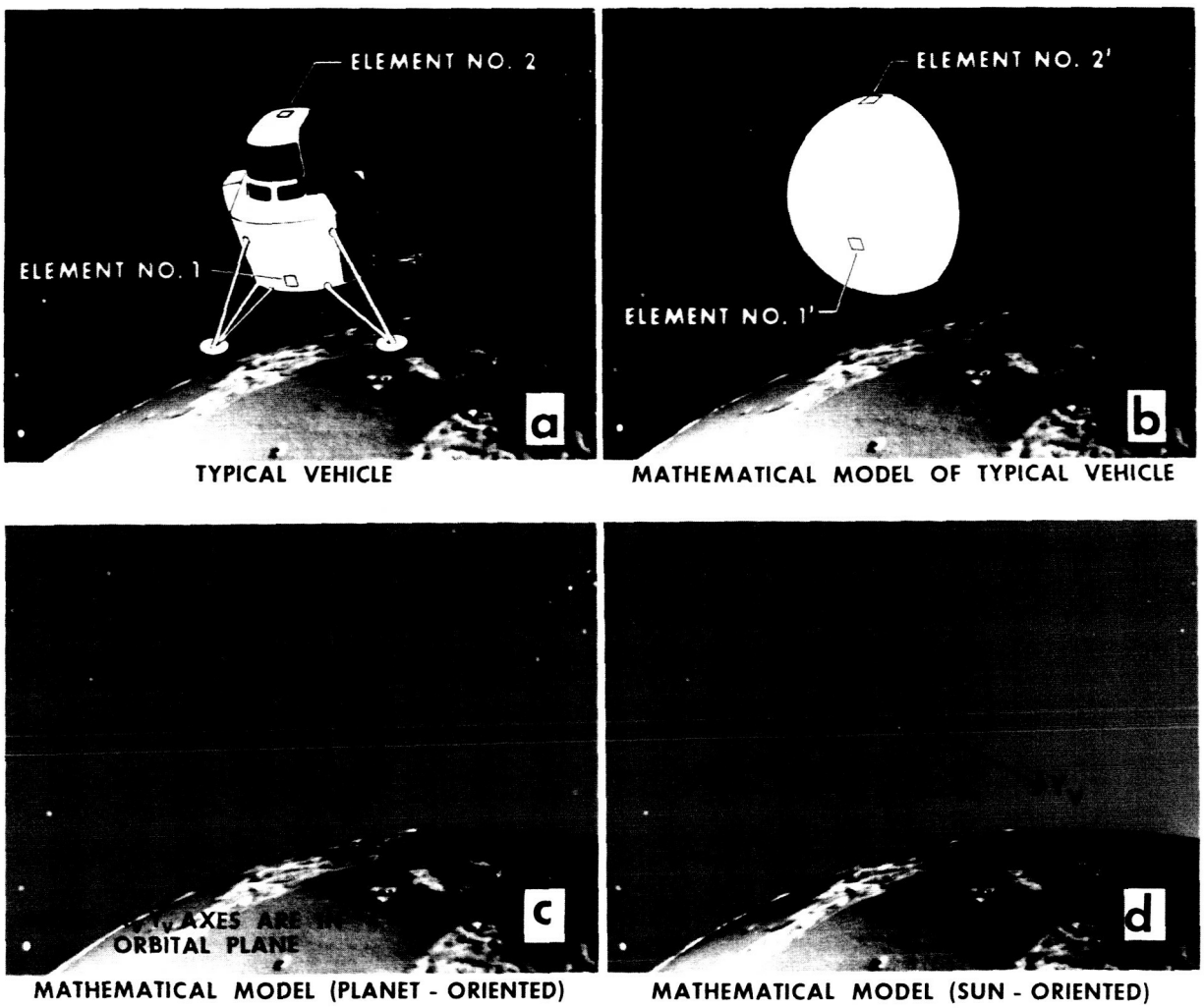

Fig. 1 - Vehicle Coordinate System for a Typical Spacecraft

B. Planet Coordinates

Before computing the impinging heat loads emitted or reflected by the planet, the second question (where is the vehicle with respect to the planet being orbited?) must be answered. The orbit and planet shown in Figs. 2a and 2b are the same; however, the latter shows the orbit rotated into the plane of the page. Superimposing the X_p and Y_p axes (planet coordinates) onto the orbit plane simplifies the equations of motion by reducing the problem from three dimensions to two. The position of the vehicle can be defined in this system by polar or cartesian coordinates.

The polar coordinates of a point on the orbit are the true anomaly, ϕ , and the distance from principal focus or center of force to the vehicle, D . The distance is given by

$$D = a(1-e \cos E) \tag{1}$$

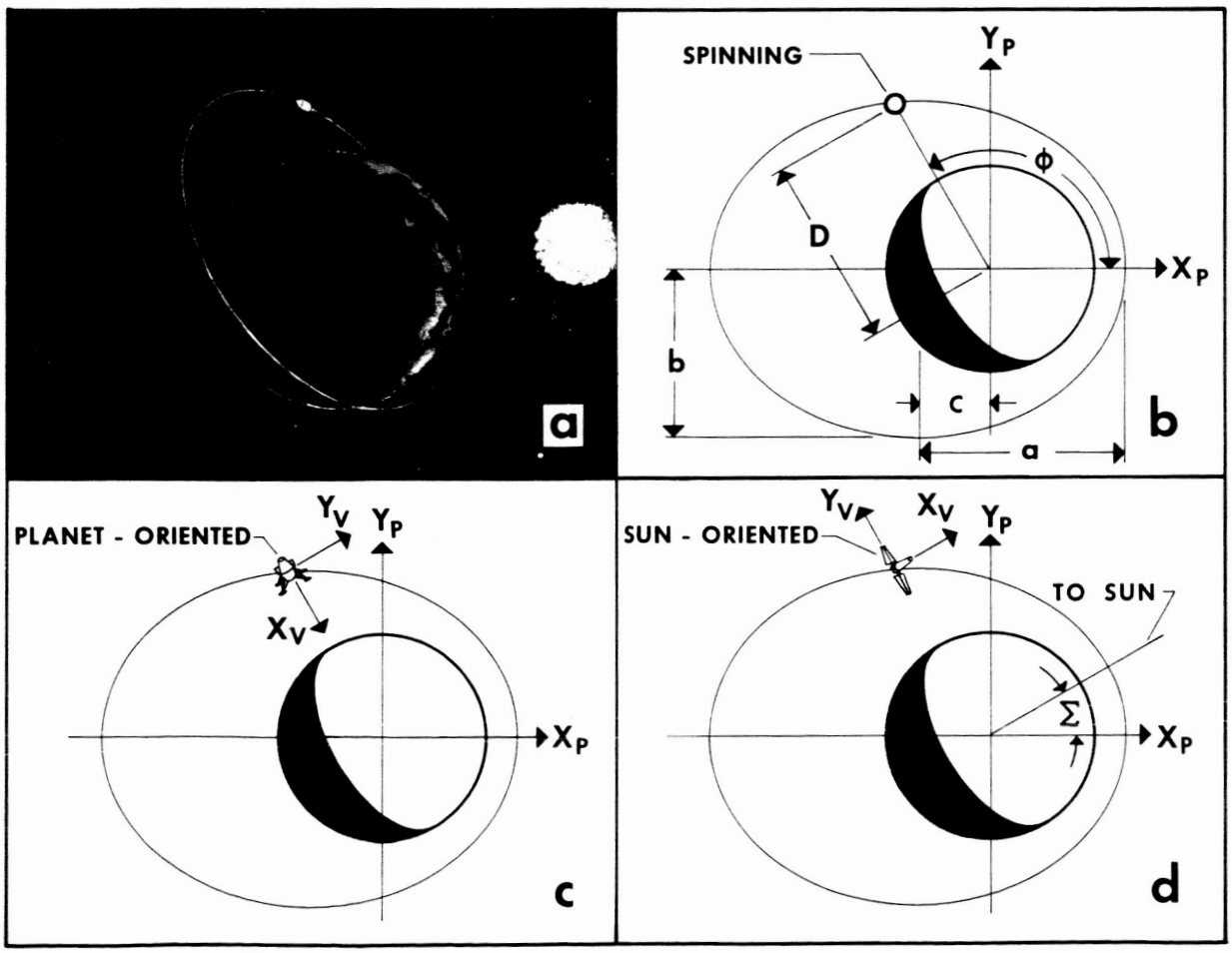

Fig. 2 - Planet Coordinate Systems for Spinning and Oriented Vehicles

where a is the semimajor axis, e is the orbit's eccentricity, and E is the eccentric anomaly. These variables are formulated as

$$e = \frac{(a^2-b^2)^{\frac{1}{2}}}{a} = \frac{c}{a} \tag{2}$$

$$E = 2 \tan^{-1} \left[\left(\tan \frac{\phi}{2}\right)\left(\frac{a-c}{b}\right) \right] \tag{3}$$

where b is the semimajor axis and c is the distance between the ellipse's center and focus.

The cartesian coordinates of a point on the orbit are X_p and Y_p and are expressed as

$$X_p = a(\cos E - e) \tag{4}$$

$$Y_p = a(1-e^2)^{\frac{1}{2}} \sin E \tag{5}$$

Vehicle coordinates for a planet-oriented orbiting body superimposed on the planet coordinate system are shown in Fig. 2c. As the vehicle makes one counterclockwise revolution about the planet, the X_v-Y_v axes similarly rotate about the Z_v axis.

Vehicle and planet coordinates are illustrated for sun-oriented satellites in Fig. 2d. The X_v-Y_v plane is generally not in the X_p-Y_p plane since X_v is directed toward the sun. These vehicle coordinates have a fixed orientation in space (assuming the planet is stationary with respect to the sun, which is essentially true during the time it takes to complete several orbits).

C. Celestial Coordinates

In order to determine the sun's contribution to spacecraft heating, the third question (what is the celestial location of the vehicle?) will be answered with respect to celestial coordinates X_c, Y_c, Z_c; but first two astronomical terms, ecliptic and vernal equinox, will be introduced.

Positions in the solar system are commonly defined with respect to the ecliptic and the vernal equinox. The ecliptic is the plane described by earth as it orbits the sun. The vernal equinox, symbolized by ♈, is a fixed line[a] from earth directed toward the sun at the instant the sun "crosses" the earth's equator from south to north in its apparent annual motion along the ecliptic.

Thus, the earth intersects the vernal equinox at the start of spring (in the northern hemisphere). The vernal equinox also lies along the line of nodes described by the intersection of the earth's equatorial plane with the ecliptic plane. The other point where the sun "crosses" the earth's equator, going from the northern to the southern hemisphere, is designated by the symbol ☊ and is the beginning of our autumn. At both points there is equal day and night.

The orbit of a vehicle about earth, another planet, or the moon is conventionally related to the celestial axes of the planet, X_c, Y_c, Z_c, by three angles Ω, ω, and i. Before these functions can be defined, it is necessary to understand the geometric relationship between the vehicle orbit and the celestial axes. In Fig. 3a the general orbit of a vehicle is shown with the intersection of the orbit plane and the planet surface shown in a broken line. The other broken line represents the intersection of the plane containing the planet axes, X_c, Y_c, with the surface of the planet. The broken lines cross at two points. (In Fig. 3a only one point is visible.) These two points define the line of intersection of the orbit plane with the plane containing the X_c, Y_c axes. The two intersections are commonly referred to as the ascending node and the descending node, while the line connecting them is called the line of nodes. The vehicle is at the ascending node when it is passing upward (north) through the X_c, Y_c plane.

The orbit and the X_c, Y_c, Z_c plane are related by Ω, ω, and i as shown in Fig. 3b. The angle Ω is the longitude of the ascending node and is measured counterclockwise in the X_c, Y_c, Z_c plane from X_c to the line of nodes. The angle ω is the argument of perifocus and is measured in the orbit plane, in the direction of travel from the line of nodes to the perigee. The angle i represents the true inclination between the X_c, Y_c plane and the orbit plane. The axes of the orbit plane are represented by X_p, Y_p, and Z_p where X_p is directed through the perigee of the orbit as previously defined.

---

a/ The direction of the vernal equinox varies slightly (approximately 50.27" per year). Hence, to specify the coordinates of an object, it is necessary to state which vernal equinox is referred to as the principal direction (e.g., the equinox of 1950 or 1965).

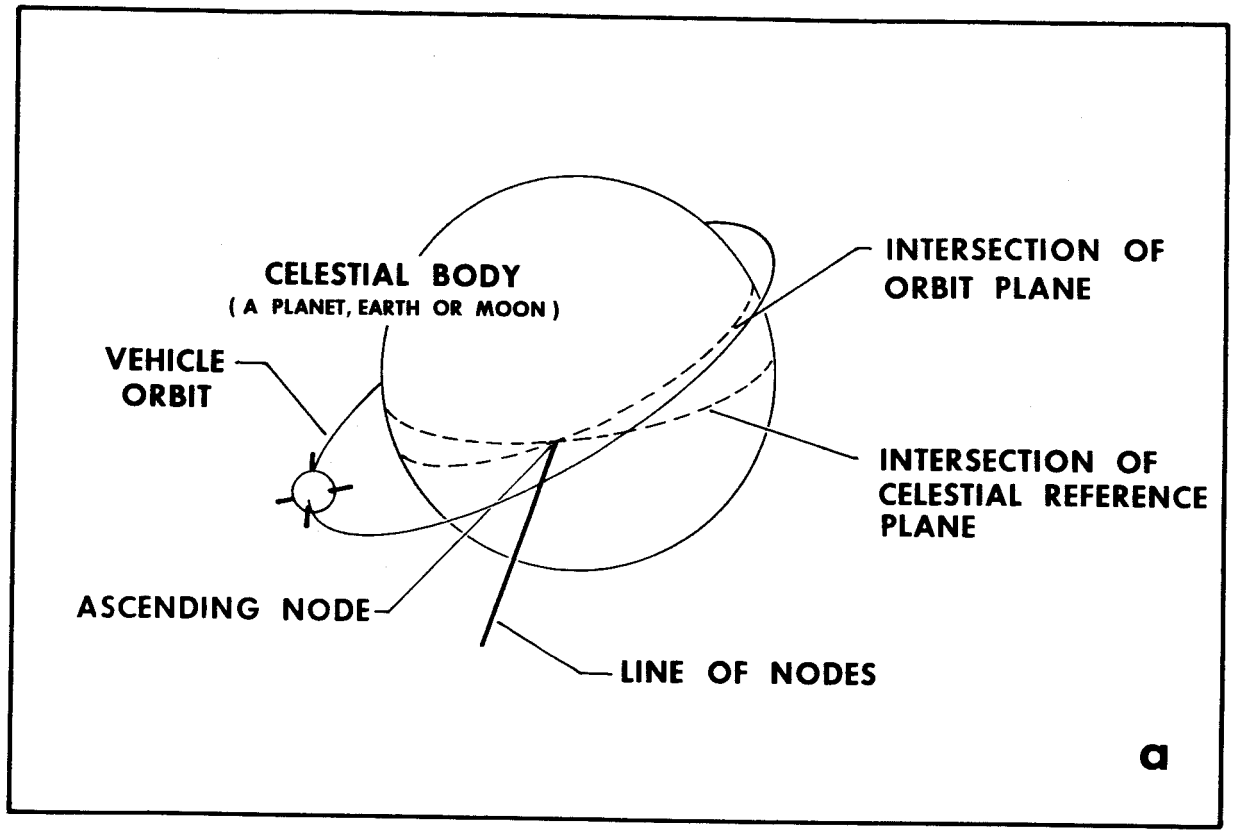

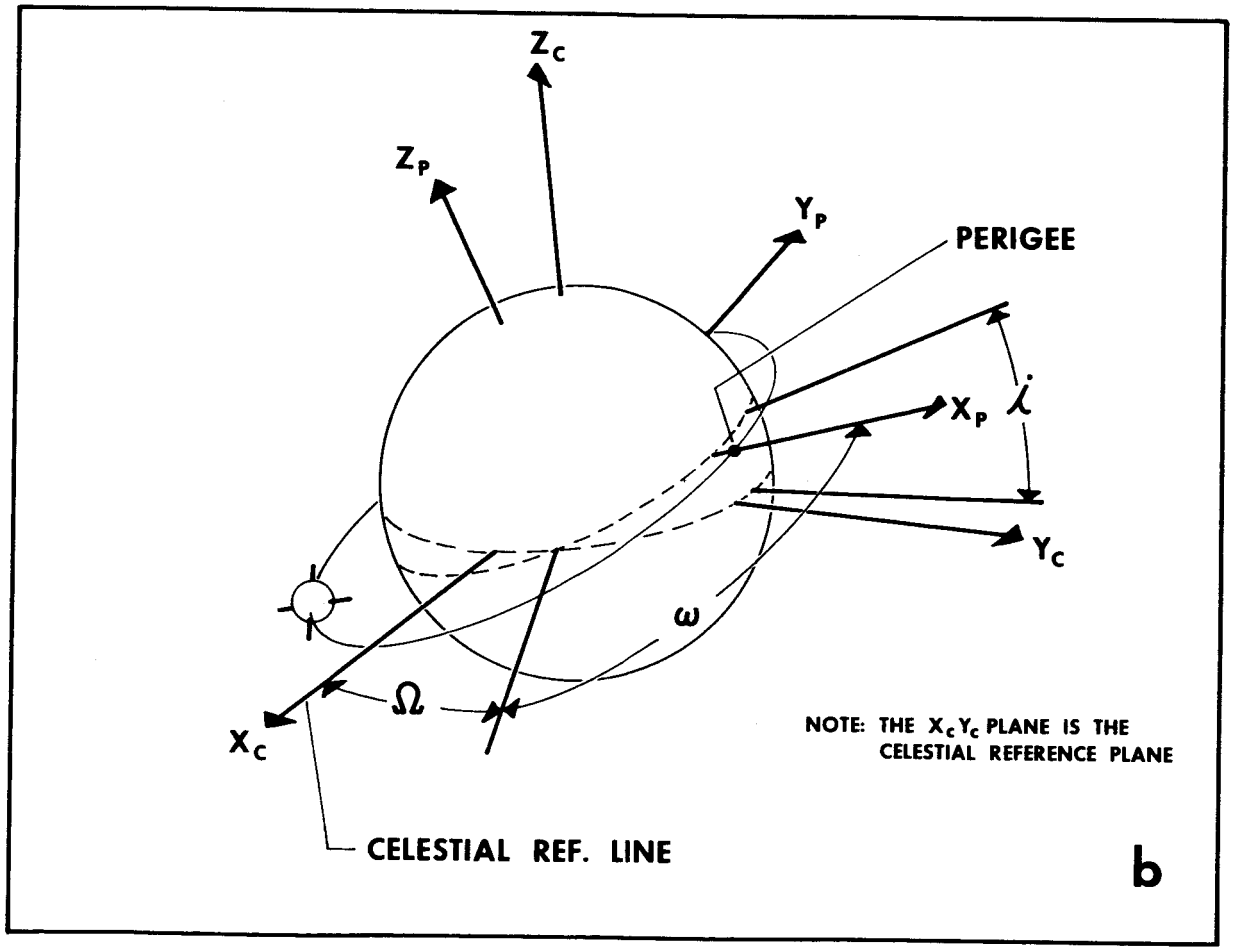

Fig. 3 - Relationship between Orbit and General Celestial Coordinate System

Any number of reference axes, X_c, Y_c, Z_c, can be chosen. The primary consideration in choosing celestial coordinate systems for this analysis was that they should be compatible with standard astronomical references so as to minimize input data compilation time and effort by the program user. Three systems, geocentric, modified heliocentric, and selenographic, were selected to describe orbits about earth, a planet other than earth, and the moon, respectively.

Conventional geocentric coordinates are employed to define orbits about earth. In this system, the X_c, Y_c reference plane is the plane of the earth's equator with the X_c axis directed along the vernal equinox as shown in Fig. 4.

A modified heliocentric coordinate system is used to define orbits about planets, other than earth. Since the equatorial planes of all planets are not well defined, the X_c, Y_c reference plane has been chosen to be parallel to the ecliptic with the X_c axis directed so as to be parallel to the vernal equinox. The X_c, Y_c, Z_c axes for planets are also illustrated in Fig. 4.

Conventional selenographic coordinates are employed to define orbits about the moon. In this system, the X_c, Y_c reference plane is in the plane of the moon's equator, and the Z_c axis extends through the north pole of the moon (see Fig. 5). The positive direction of the X_c axis is from the center of the moon out through the moon's prime meridian. By definition, the lunar prime meridian passes through the mean center of the moon. The mean center is the point on the lunar surface that is directed toward the earth's center when the moon is at the mean ascending node, and the node coincides with the mean perigee or mean apogee. The longitude is measured positive toward the west as seen by an observer on earth or in a counterclockwise direction from the X_c axis (toward Mare Crisium). The direction of the X_c axis in space is not fixed; the axis revolves with the moon, making one turn every 28 days.

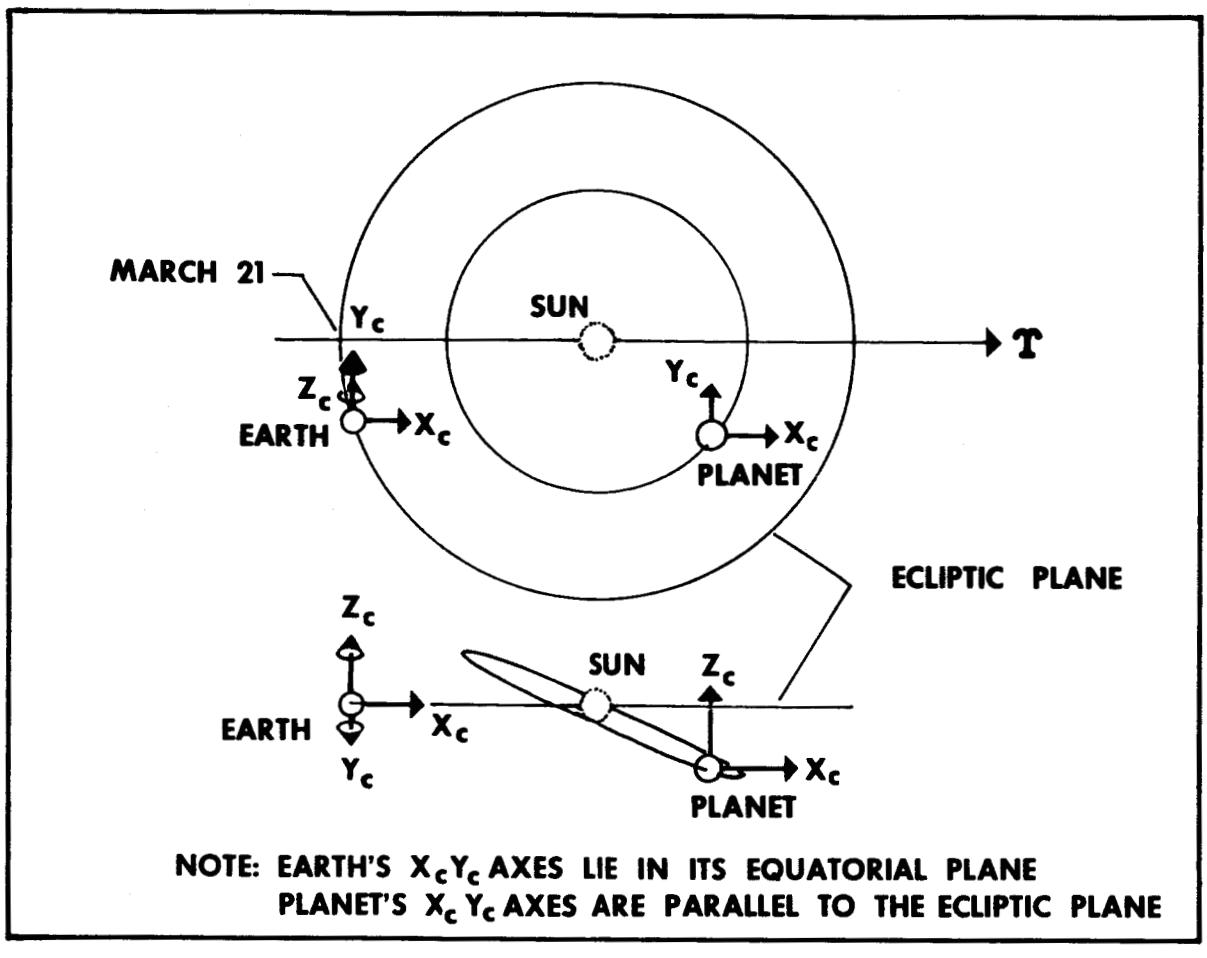

Fig. 4 - Celestial Coordinate System for Earth (Geocentric) and Other Planets (Modified Heliocentric)

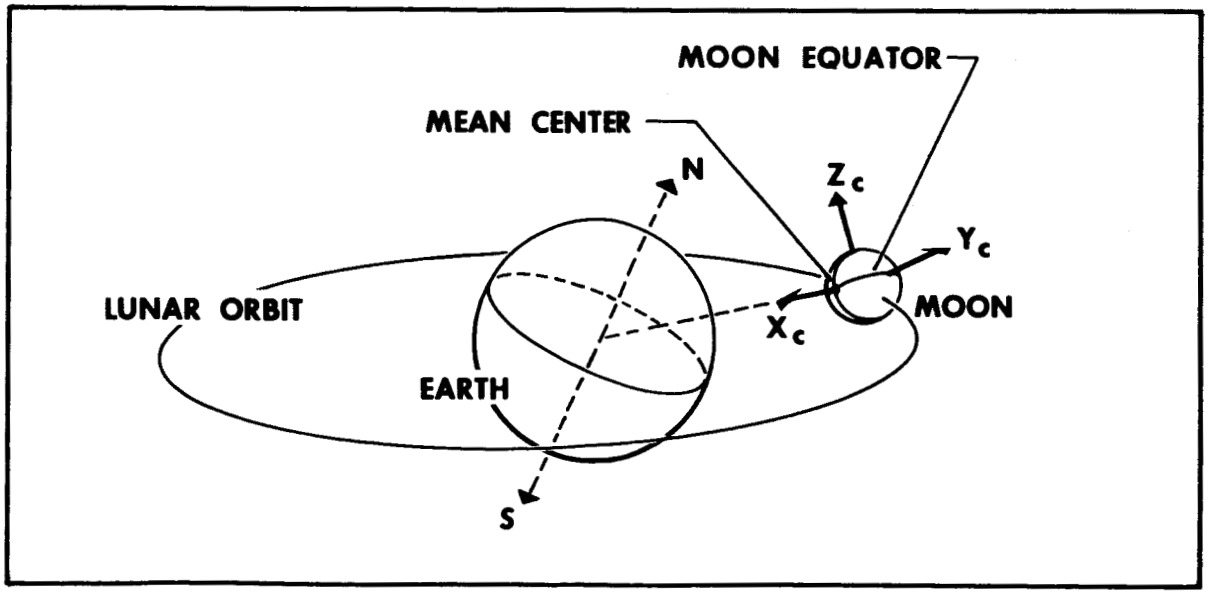

Fig. 5 - Celestial Coordinate System for the Moon (Selenographic)

D. The Sun's Position

The position of the sun can be expressed, with respect to the celestial body being orbited (in X_c, Y_c, Z_c coordinates) in terms of right ascension, RA, and declination, DEC, as shown in Fig. 6. For earth, RA and DEC can be obtained directly from an ephemerides[a] for each day of the year. For the moon, the required coordinates are listed in the ephemerides as latitude and colongitude, where colongitude is

$$\text{colongitude} = 90° - \text{longitude}$$

For any planet other than earth, the right ascension and declination of the planet with respect to the sun are given in the American Ephemeris in heliocentric coordinates. The sun's position with respect to the modified heliocentric coordinate system can be obtained from these data as demonstrated in the following examples. If the declination of the planet with respect to the sun is $\pm 10°$, the declination of the sun with respect to the planet is $-10°$. If the right ascension or longitude of the sun with respect to the planet is $236°$, the required value is $236° + 180° = 416° = 56°$.

The position of the sun can be expressed, with respect to the planet coordinate axes X_p, Y_p, Z_p in terms of α, β, and γ as shown in Fig. 7. The coordinates RA and DEC can be transformed into α, β, and γ by performing rotations through the angles Ω, ω, and i as shown in Figs. 6 and 7. The first transformation rotates the X_c axis about the Z_c axis through an angle of Ω into the line of nodes (see also Fig. 3). The second transformation rotates the Y_c axis about the X_c axis by the angle i. Finally the X_c axis is rotated through an angle of ω about the Z_c axis.

---

a/ Ephremerides is the plural form of ephemeris, which is a table of calculated coordinates of celestial bodies with equidistant dates as arguments. The data required to express the sun's position re this project can be obtained from "The American Ephemeris and Nautical Almanac."[2]

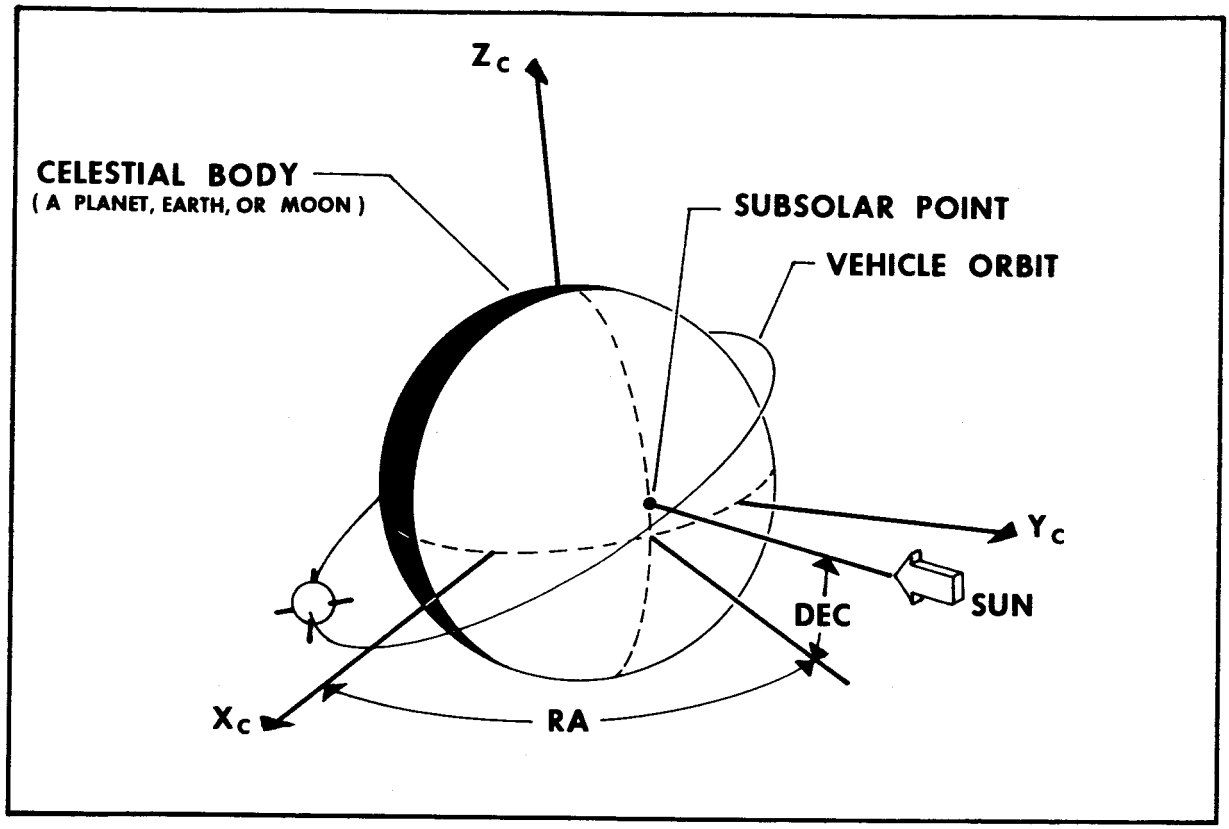

Fig. 6 - Sun's Position Relative to the Celestial Coordinate System

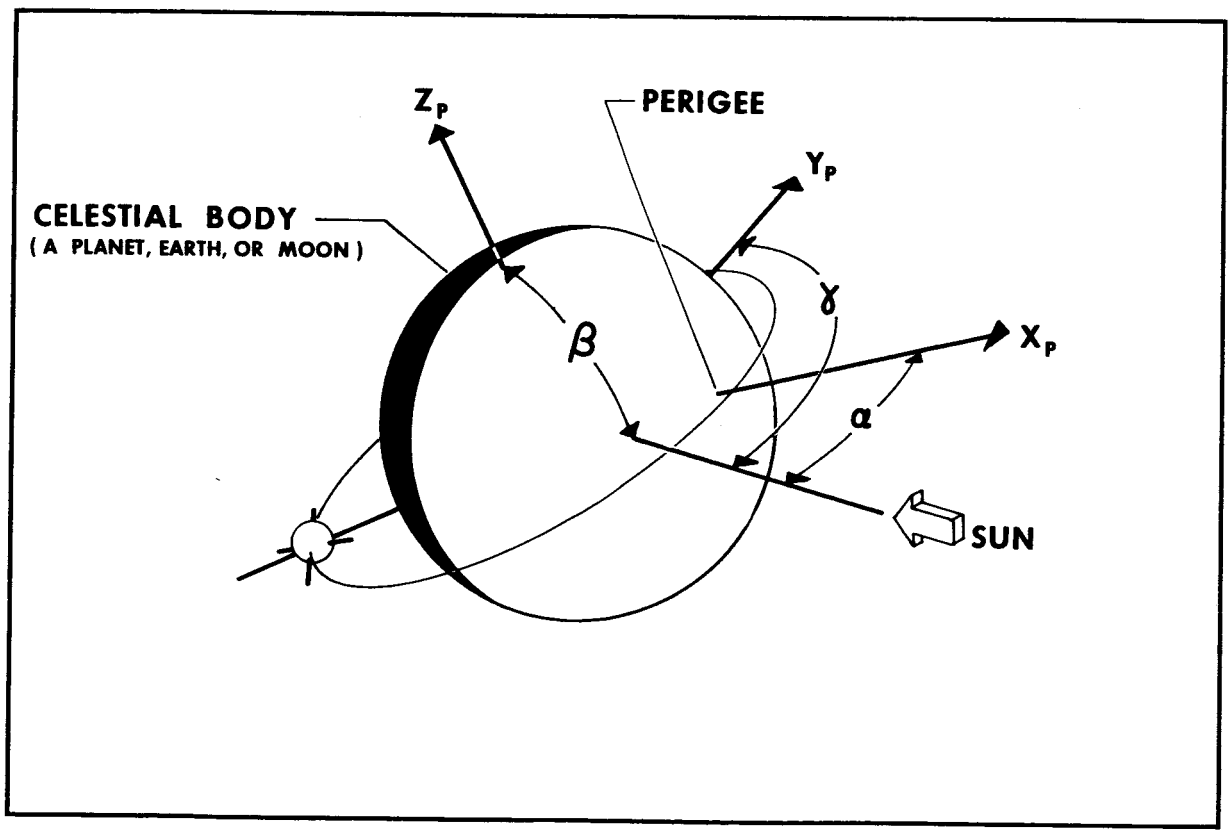

Fig. 7 - Sun's Position Relative to the Planet Coordinate System

Performing the above transformations gives the following relationships:

$$\cos \alpha = \left[(\cos \omega)(\cos \Omega)-(\sin \omega)(\sin \Omega)(\cos i)\right](\cos RA)(\cos DEC)$$

$$+ \left[(\cos \omega)(\sin \Omega)+(\sin \omega)(\cos \Omega)(\cos i)\right](\sin RA)(\cos DEC)$$

$$+ (\sin \omega)(\sin i)(\sin DEC) \tag{6}$$

$$\cos \gamma = \left[(-\sin \omega)(\cos \Omega)-(\cos \omega)(\sin \Omega)(\cos i)\right](\cos RA)(\cos DEC)$$

$$+ \left[(-\sin \Omega)(\sin \omega)+(\cos \Omega)(\cos \omega)(\cos i)\right](\sin RA)(\cos DEC)$$

$$+ (\cos \omega)(\sin i)(\sin DEC) \tag{7}$$

$$\cos \beta = (\sin \Omega)(\sin i)(\cos RA)(\cos DEC)$$

$$+ (-\cos \Omega)(\sin i)(\sin RA)(\cos DEC)+(\cos i)(\sin DEC) \tag{8}$$

For clarity, the derivations of the above equations have been omitted.

The sun's position with respect to the planet and the orbit plane having been obtained, the final step is to determine its location in relation to the orbiting spacecraft. This determination is accomplished below for spinning and planet- and sun-oriented vehicles.

1. <u>Sun's position with respect to spinning vehicles</u>: Some of the solar energy that strikes the planet and its atmosphere is scattered back into space and impinges on the orbiting vehicle. This radiation, albedo, travels through the angle θ_s, which is shown in Fig. 11. Cos θ_s is equal to the sum of the direction cosines of the planet-vehicle line times that of the sun-planet line which reduces to

$$\cos \theta_s = \frac{X_p}{D} \cos \alpha + \frac{Y_p}{D} \cos \gamma \tag{9}$$

Solar energy directly irradiating the vehicle is the same throughout the orbit (except when shaded by the planet) if it is assumed that the period of rotation of the spinning sphere is short (i.e., all surface elements continuously "see" the sun), and it is assumed that the sun is a point source infinitely far away. Therefore, no other angles relating the sun's position to the vehicle are required.

2. Sun's position with respect to planet-oriented vehicles: The angles (Ω_s, Λ_s, and δ) illustrated in Fig. 8 and θ_s define the relative positions of the sun, vehicle, vehicle element and planet. Cos θ_s is the same as for a spinning sphere and is given in Eq. (9).

Since Z_v is parallel to Z_p (see Fig. 2c) and since it is assumed that the sun is a point source infinitely far away, it follows that

$$\Omega_s = \beta \tag{10}$$

It can also be shown that

$$\Lambda_s = \Sigma - \phi + \pi \tag{11}$$

where Σ is the true anomaly of the sun's projection on the X_p, Y_p plane and is shown in Fig. 2.[a]

The angle δ between the element-vehicle line and the sun-vehicle lines is derived by adding the products of the corresponding direction cosines of the two lines which give

$$\cos \delta = \sin \Omega \cos \Lambda \sin \Omega_s \cos \Lambda_s$$

$$+ \sin \Omega \sin \Lambda_s \sin \Omega_s \sin \Lambda_s + \cos \Omega \cos \Omega_s \tag{12}$$

---

a/ 2π radians should be added to Λ_s if it is negative. However, only $\sin \Lambda_s$ and $\cos \Lambda_s$ are required by the analysis; therefore, Eq. (11) need not be modified for negative values.

3. Sun's position with respect to sun-oriented vehicles: The angle θ_s is independent of vehicle orientation; therefore, it is the same as expressed in Eq. (9).

By definition, the X_c axis is directed toward the sun; therefore,

$$\Omega_s = \pi/2 \tag{13}$$

$$\Lambda_s = 0 \tag{14}$$

as shown in Fig. 9.

The angle between the element-vehicle line and the sun-vehicle line, δ , can be derived by combining Eqs. (12), (13), and (14), which yields

$$\cos \delta = \sin \Omega_s \cos \Lambda_s \tag{15}$$

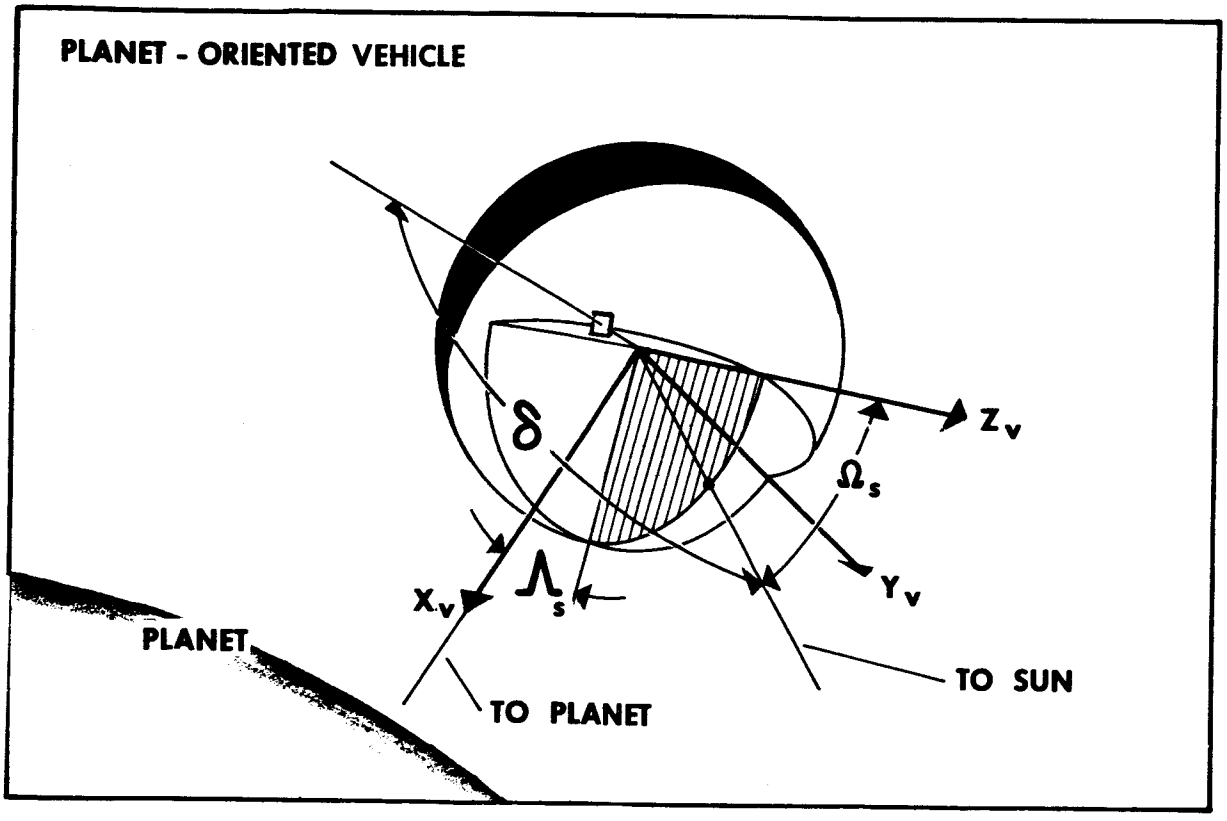

Fig. 8 - Sun's Position Relative to the Vehicle Coordinate System (Planet-Oriented)

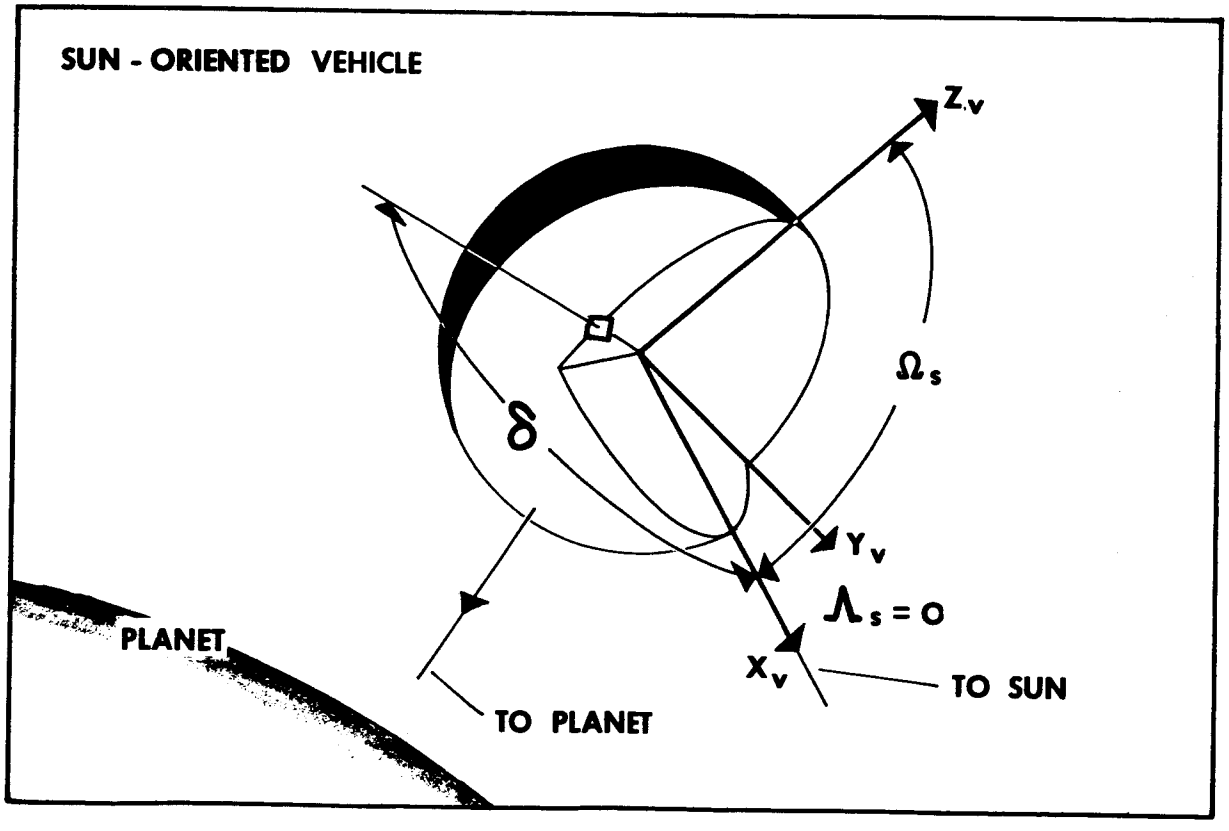

Fig. 9 - Sun's Position Relative to the Vehicle Coordinate System (Sun-Oriented)

Table

Summary of Coordinate Systems

A. Vehicle Coordinate System

Vehicle Orientation	Origin of Axis	Location of X_v	Location of Y_v	Location of Z_v	Location of Surface Element
Planet-oriented	Vehicle mass center	Line connecting centers of vehicle and planet, positive direction toward planet	In the orbit plane at right angles to X_v axis	Normal to orbit plane to form a right-handed coordinate system	Λ' measured from X_v toward Y_v and Ω' measured from Z_v
Sun-oriented	Vehicle mass center	Line connecting centers of vehicle and sun, positive direction toward sun	In the orbit plane at right angles to X_v axis	To form a right-handed coordinate system	Λ' measured from X_v toward Y_v and Ω' measured from Z_v
Spinning	X_v, Y_v, Z_v axes are not applicable to spinning vehicles				

B. Planet Coordinate System

Vehicle Orientation	Origin of Axis	Location of X_p	Location of Y_p	Location of Z_p	Location of Vehicle: Cartesian Coordinates	Location of Vehicle: Polar Coordinates
All	At mass center of celestial body being orbited	Along major axis of orbit, positive direction toward perigee	Along minor axis of orbit	To form a right-handed coordinate system	X_p and Y_p (may be + or -)	ϕ, true anomaly and D, distance from principal focus to vehicle

C. Celestial Coordinate System

Vehicle Orientation	Coordinate Basis	Location of X_c	Location of Y_c	Location of Z_c	Location of Sun
About earth	Geocentric, ♈ reference, center at earth	Positive X_c toward vernal equinox	Perp. to X_c in plane of earth's equator	To form a right-handed coordinate system	From ephemeris, geocentric coordinate system, apparent right ascension and apparent declination
About the moon	Selenographic, moon's prime meridian reference, center at moon	Positive along line connecting moon and earth	Perp. to X_c in plane of moon's equator	To form a right-handed coordinate system	From ephemeris, in selenographic coordinate system, colongitude and latitude of sun
About a planet	Modified heliocentric, ♈ reference, center at planet	Parallel to heliocentric X axis, positive toward ♈	Perp. to X_c in plane parallel to ecliptic	To form a right-handed coordinate system	Ephemeris gives planet's position with respect to sun. Add 180° to longitude and change sign of latitude to obtain sun's position with respect to planet

III. HEAT TRANSFER THEORY

Methods for determining impinging heat loads and transient surface temperatures of spacecraft are based on fundamental heat transfer theory. These methods and appropriate equations are summarized below. Detailed derivations are given in the Appendices.

A. Heat Loads

A vehicle orbiting in a vacuum is externally heated by radiation. It is principally irradiated by the planet it orbits and by the sun. The amount of heat originating from other celestial bodies is negligible. Most of the solar radiation comes directly from the sun, the remainder is reflected by the planet before impinging the vehicle's surface. Solar, planet, and albedo heat fluxes are illustrated in Fig. 10.

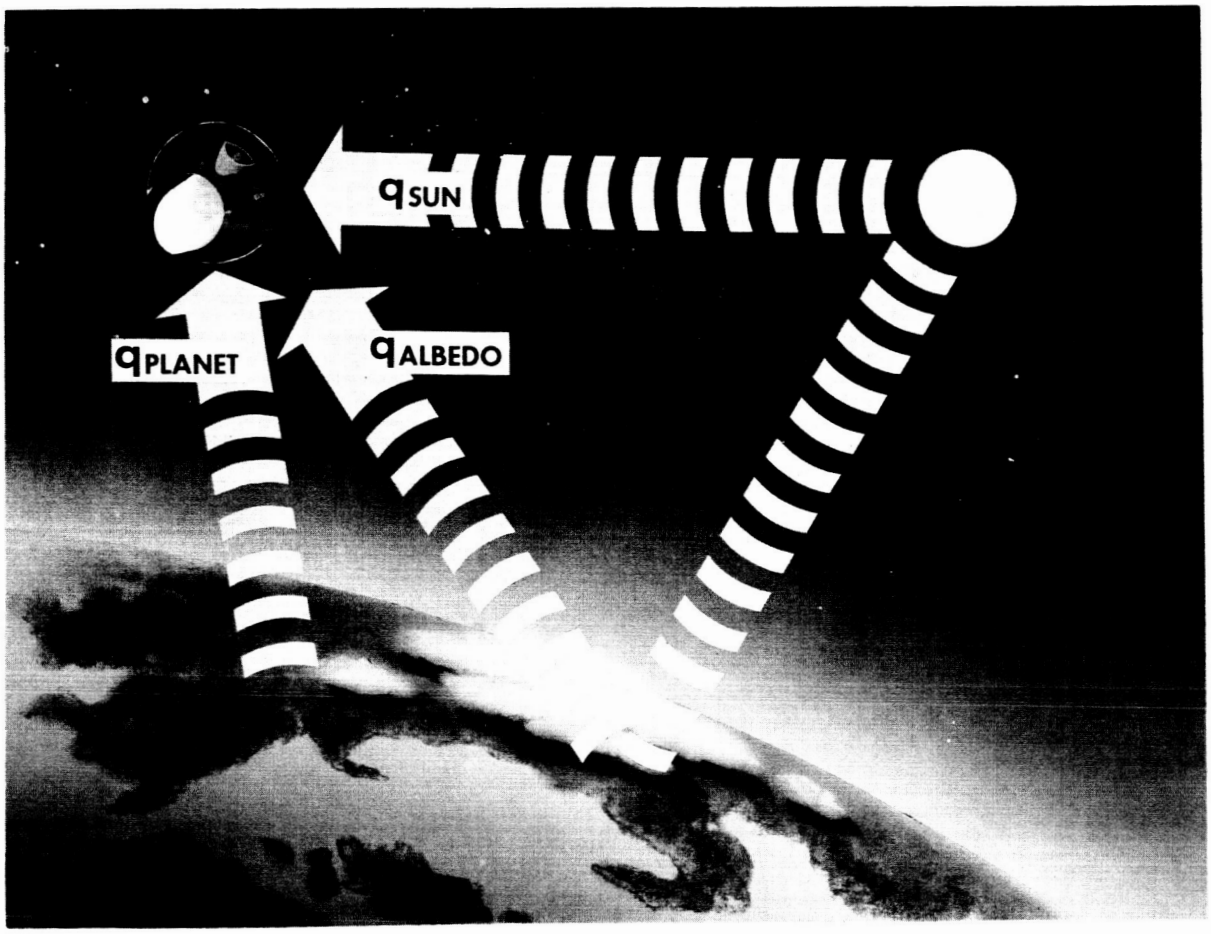

Fig. 10 - Principal External Heat Loads

Since an orbiting vehicle may spend much of its time in the planet's shadow during which time it is shielded from both direct and reflected solar radiation, it is necessary to know what part of the orbit is shaded. An analysis for determining the intersection of the orbit and the shadow is described in Appendix A.

Planet-emitted heat is dependent on the source's surface temperature. If the celestial body is shrouded with a heavy atmospheric blanket, its surface temperature is relatively uniform due to convection and conduction heat transfer and can be considered to be constant. It is impractical if not impossible to account for temperature deviations from the average, since they are functions of such intangibles as the wind, snow, cloud coverage, and atmospheric activity.

If the celestial body has a negligible atmosphere and a nonconducting surface (like the moon), the temperature gradients are large and should be accounted for. Fortunately, the factors that cause these extreme variations also make it possible to determine the surface temperature distribution with reasonable accuracy.

External heat loads are summarized below for spinning and oriented vehicles as functions of altitude and the parameters, θ_s , Ω', Λ' , Ω_s, Λ_s, δ , which were previously described (see pp. 10 and 20), as well as two variables, ϵ and ϕ_c , yet to be defined. Complete derivations are given in Appendix B.

1. <u>Radiation impinging spinning vehicles</u>: Solar radiation per cross-sectional area, A_v , striking a spinning vehicle is

$$\frac{q_{solar}}{A_v} = S \tag{16}$$

where S is the solar "constant" which varies in space inversely proportional to the square of the distance from the sun.

Radiation received from a constant temperature ($T_p = C$) planet is given in Eq. (B-16) as

$$\frac{q_{planet}}{A_v} = 2S(1-R)F_1 \ , \ T_p = C \tag{17a}$$

where

$$F_1 = \frac{1 - \left[1 - \left(\frac{r_p}{D}\right)^2\right]^{\frac{1}{2}}}{\cancel{8}\ 4} \tag{17b}$$

The corresponding variable temperature $(T_p \neq C)$ planet heat rate is expressed in Eq. (B-30) as

$$\frac{q_{planet}}{A_v} = 8S(1-R)F_2 \ , \ T_p \neq C \tag{18a}$$

where

$$F_2 \approx \left\{ \frac{1 - \left[1 - \left(\frac{r_p}{D}\right)^2\right]^{\frac{1}{2}}}{\cancel{8}\ 4} \right\} \cos\ \theta_s \tag{18b}$$

closely approximates the exact configuration factor as demonstrated in Fig. B-5.

The dark side of a variable temperature planet approaches absolute zero; however, it does emit some heat, which according to Eq. (B-33) is

$$\frac{q_{planet}}{A_v} = \overset{8}{\cancel{16}}\sigma T_m^4 F_1 \ ; \ T_p \neq C \text{ (dark side of planet)} \tag{19}$$

where F_1 is defined in Eq. (17b), σ is the Stefan-Boltzmann constant, and T_m is the average dark side or minimum planet temperature. Values of T_m for all of the planets are internally stored in the computer program even though they are not very meaningful for planets that have relatively uniform surface temperatures. The "variable temperature" method should be used only for planets like the moon. The choice of method, which is left to the program user, is discussed in Section V (see also p. 25).

The albedo heat flux impinging on a spinning vehicle is given in Eq. (B-38) as

$$\frac{q_{albedo}}{A_v} = 8\ SR\ F_2 \tag{20}$$

where F_2 is defined in Eq. (18b).

2. Radiation impinging on oriented vehicles: The incident heat flux on an oriented vehicle can vary considerably from one surface position to another; therefore, thermal equations must be derived that are applicable to any spacecraft element (see Fig. 1). The equations developed in Appendix B are applicable to either sun-oriented or planet-oriented vehicles provided the required independent variables (e.g., δ) are defined for each orientation as described in Section II. The formulas are developed for a typical surface element which is located with respect to the vehicle coordinate system by the angles Λ' and Ω' as shown in Fig. 1c and Fig. 1d.

Solar radiation impinging on a surface element is

$$\frac{q_{sun}}{A_v} = S \cos \delta\ ,\ \delta \leq 90^\circ \tag{21a}$$

If δ, which was shown in Fig. 8, is greater than 90° (i.e., $\cos \delta < 0$), the element does not "see" the sun, therefore

$$\frac{q_{sun}}{A_v} = 0\ ,\ \delta > 90^\circ \tag{21b}$$

The heat flux from a constant temperature planet is given in Eq. (B-46) as

$$\frac{q_{planet}}{A_v} = \frac{S(1-R)F_4}{4}\ ,\ T_p = C \tag{22}$$

where F_4 is a function of altitude, H , and the variables ϕ_c and ϵ which are illustrated in Fig. 11. Values of F_4 have been evaluated by numerical integration over the applicable ranges of ϕ_c and ϵ and to an altitude where the configuration factor, and therefore the planet heat, is negligible (an altitude of approximately five planet radii).[a] A table of over 2,500 values representing the function $F_4 = f(\phi_c, \epsilon, \text{ and } H)$, has been incorporated into the computer program, but for simplicity the table is not included in this report.

---

a/ $F_4(H = 5r_p) \leq \left[0.015\right] \cdot \left[F_4(H = 0)\right]$ for all values of ϕ_c and ϵ .

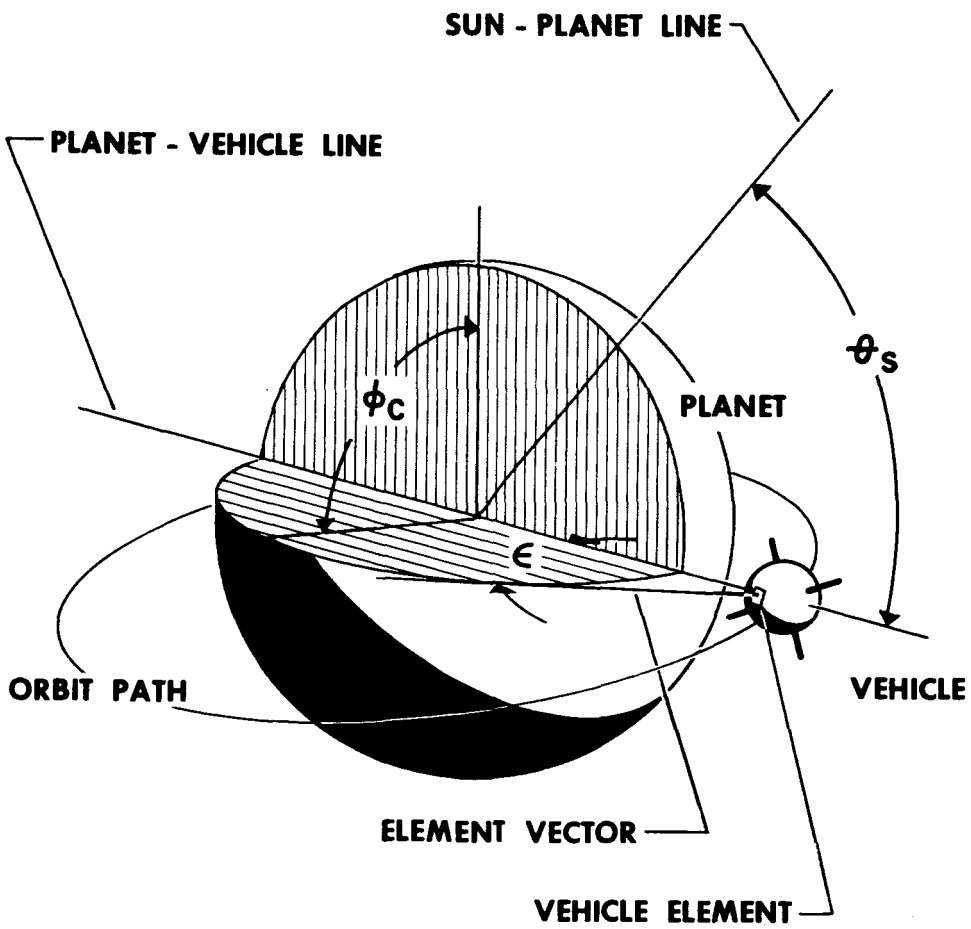

Fig. 11 - Angular Variables for Determining Configuration Factors of Oriented Vehicles

The heat flux from a variable temperature planet is given in Eq. (B-42) as

$$\frac{q_{planet}}{A_v} = S(1-R)F_3 \ , \ T_p \neq C \tag{23}$$

where F_3 is a function of H , ϕ_c , ϵ , and θ_s . The variable θ_s is the angle between the vehicle, the planet, and the sun as shown in Fig. 11. Appendix B describes in detail the relationship that exists between F_3 and F_4 .

The impinging heat from the dark side of a variable temperature planet is given in Eq. (B-47) as

$$\frac{q_{planet}}{A_v} = \sigma T_m^4 F_4 \ ; \ T_p \neq C \text{ (dark side of planet)} \tag{24}$$

The albedo heat flux irradiating an oriented vehicle element is expressed in Eq. (B-50) as

$$\frac{q_{albedo}}{A_v} = SR\ F_3 \tag{25}$$

B. Transient Temperatures

The transient temperature of an orbiting vehicle is obtained by conducting a heat balance on it and by solving the resulting differential equation. The scope of work of this project is such that all surface elements of oriented vehicles are considered to be thermally isolated from each other.

The general governing differential equation is

$$\frac{dT}{dt} = \frac{1}{\rho C_p V}(q_{sun} + q_{albedo} + q_{planet} + q_{internal} - q_{out}) \tag{26}$$

where ρ and C_p are the density and the specific heat, respectively, of the vehicle material and V is the volume being analyzed. The term, $q_{internal}$, represents the amount of internally generated heat that is absorbed by the vehicle skin. It is assumed that $q_{internal}$ is dissipated uniformly over the entire vehicle external area if it is spinning or similarly distributed over the element surface if the spacecraft is planet- or sun oriented. Internally generated heat is expressed as

$$q_{internal} = Q_g \tag{27}$$

The negative term in Eq. (26), q_{out}, is the heat emitted by the vehicle and is given by

$$\frac{q_{out}}{A_T} = \sigma \, \epsilon_v T^4 \tag{28}$$

where T is the instantaneous surface temperature and ϵ_v is the material's emissivity at temperature T, and A_T is the total emitting surface area.

The external heat fluxes, q_{sun}, q_{albedo}, and q_{planet}, have been derived for spinning and oriented vehicles with respect to constant and variable temperature planets (see pp. 25 through 29).

Introducing the appropriate heat terms into Eq. (26) gives the governing temperature differential equations.

For a spinning vehicle orbiting a constant temperature planet:

$$\frac{dT}{dt} = \frac{1}{\rho C_p h}\left[\frac{S\alpha_s}{4} + 2SR\,\alpha_s F_2 + \frac{S(1-R)\alpha_p F_1}{2} + Q_g - \sigma\,\epsilon_v T^4\right] \tag{29a}$$

where h is skin thickness and α_s and α_p are the material's absorptivity with respect to solar and planet radiation, respectively. According to Kreith,[3] a noted author in the field of radiation heat transfer and spacecraft thermal control, a material's absorptivity is a function of the source temperature, but is independent of the receiver's temperature.

For a spinning vehicle orbiting a variable temperature planet:

$$\frac{dT}{dt} = \frac{1}{\rho C_p h}\left[\frac{S\alpha_s}{4} + 2SR\ \alpha_s F_2 + 2S(1-R)\alpha_p F_2 + Q_g - \sigma\ \epsilon_v T^4\right] \tag{29b}$$

or

$$\frac{dT}{dt} = \frac{1}{\rho C_p h}\left[\frac{S\alpha_s}{4} + 2SR\ \alpha_s F_2 + 2\sigma\ \alpha_p T_m^4 F_1 + Q_g - \sigma\ \epsilon_v T^4\right] \tag{29c}$$

depending on whether the vehicle is above the sunlit or dark side of the planet, respectively. Near the terminator the larger value of dT/dt from Eqs. (29b) and (29c) is used.

For an oriented vehicle orbiting a constant temperature planet:

$$\frac{dT}{dt} = \frac{1}{\rho C_p h}\left[S\alpha_s \cos\delta + SR\ \alpha_s F_3 + \frac{S(1-R)\alpha_p F_4}{4} + Q_g - \sigma\ \epsilon_v T^4\right] \tag{29d}$$

For an oriented vehicle orbiting a variable temperature planet:

$$\frac{dT}{dt} = \frac{1}{\rho C_p h}\left[S\alpha_s \cos\delta + SR\ \alpha_s F_3 + S(1-R)\alpha_p F_3 + Q_g - \sigma\ \epsilon_v T^4\right] \tag{29e}$$

or if the oriented vehicle is above the shaded half of the planet:

$$\frac{dT}{dt} = \frac{1}{\rho C_p h}\left[S\alpha_s \cos\delta + SR\ \alpha_s F_3 + \sigma T_m^4 \alpha_p F_4 + Q_g - \sigma\ \epsilon_v T^4\right] \tag{29f}$$

Near the terminator Eqs. (29e) and (29f) are both evaluated, but the smaller value of dT/dt is discarded.

The above equations are of the form

$$\frac{dT}{dt} = C_1 - C_2T^4 \tag{30}$$

where C_1 and C_2 are variable coefficients. Both t and ϕ must be known in order to evaluate C_1 and C_2, thus an expression relating t and ϕ is required. The necessary relationship is derived by first writing t as a function of the eccentric anomaly, E, in accordance with Kepler's laws of planetary motion:

$$t = \frac{(E-e \sin E)P}{2\pi} \tag{31}$$

where t as well as E is measured from perigee. The period, P, is

$$P = 2\pi\left(\frac{a^3}{GM_p}\right)^{\frac{1}{2}} \tag{32}$$

where G is a gravitational constant and M_p is the planet mass.

Time can now be expressed as a function of ϕ by combining Eqs. (3), (31), and (32) which yields

$$t = \frac{2 \tan^{-1}\left[\left(\tan\frac{\phi}{2}\right)\left(\frac{a-c}{b}\right)\right] - e \sin\left\{2\tan^{-1}\left[\left(\tan\frac{\phi}{2}\right)\left(\frac{a-c}{b}\right)\right]\right\}}{2\pi P^{-1}} \tag{33}$$

The above expression can readily be solved for t; however, the solution of $\phi = f(t)$ requires some kind of iterative technique. Consequently, ϕ has been selected as the independent variable. This is indicated in the general differential equation, Eq. (30), as follows:

$$\frac{dT}{d[t(\phi)]} = C_1 - C_2T^4 \tag{34}$$

Equation (34) does not yield a closed form solution, but it can be solved numerically. The procedure for numerically integrating this equation is described in Section IV, "Numerical Analysis."

IV. NUMERICAL ANALYSIS

It is important that numerical techniques be both accurate and fast. The accuracy and speed of numerically integrating an equation such as the general thermal expression, Eq. (34), are related to the specific method and step-size to be used as well as to the function itself. Of course, accuracy also depends on proper application of the numerical technique employed.

A. Method of Integration

Multistep methods require a constant step-size, and although they are generally faster than single-step methods, their use for this specific problem would necessitate a time-consuming iterative solution of Eq. (33) to find the true anomaly increment corresponding to the constant time increment (see p. 12). Consequently, a single-step integration method should be chosen.

An analysis of single-step methods in relation to the general equation to be solved resulted in the selection of the fourth-order Runge-Kutta technique. This method has long been accepted as being generally best in terms of accuracy and speed. In the case of Eq. (34), it is particularly well suited in the sense of speed since C_1 and C_2 need to be calculated only once during each time interval. Because of this, the integration speed of the fourth-order Runge-Kutta method is very close to that of a lower-ordered method, or, for that matter, even the multistep methods that are normally much faster.

B. Step-Size and Error Analysis

Assuming that the error attributable to a given single-step method is less than the maximum tolerable error, operating speed can be optimized by investigating the question of maximum step-size.

The computer program has been written so that the user can input a step-size, $\Delta\phi$. The program prints out every $n \cdot \Delta\phi$ intervals, where n is a specified integer; however, calculations may be based on a smaller, more "practical"[a] interval re accuracy, speed, and stability. The practicality of $\Delta\phi$ is determined at the start of each interval.

---

a/ Practical step-size and its determination by the program are described in Appendix C.

The errors induced by numerical integration can be broken down in the following manner:

$$E_n = e_{t,n} + e_{t,a} + e_{ro} \tag{35}$$

where E_n = total error at $t = n$

$e_{t,n}$ = one-step truncation error (the error due to approximation over step n)

$e_{t,a}$ = accumulated truncation error over steps 1 to $n-1$

e_{ro} = accumulated effect of round-off error over n steps

1. Accumulated errors, e_{ro} and $e_{t,a}$: Contrary to the usual case in numerical analysis, the sum of the accumulated errors, $e_{t,a}$ and e_{ro} , is bounded by some number, ε , which is much less than the accuracy of the input data for any practical step-size and, therefore, negligible regardless of total integration time. The reason for this boundedness is the stability of the function to be integrated; in other words, the solution converges to a specific temperature at a given true anomaly and, on all subsequent orbits, will be virtually at that temperature. Since the temperature at point n in one orbit is the same as the temperature at point n in the next orbit, there is no significant accumulation of errors.

To test this reasoning, the spinning case was programmed for the IBM 1620 so that $e_{t,a}$ and e_{ro} could be analyzed separately. To show that e_{ro} was nearly zero, the program was run using 8-digit accuracy, then it was run using 12-digit accuracy. The difference in the two solutions was in the seventh or eighth place in all of the many orbits that were run.

The analysis included the calculation of a function proven[4] to be asymptotic to the accumulated truncation error of the integration. Although the solution of this function was small with respect to the solution of the thermal equation, and was oscillatory in nature, it did gradually increase in magnitude. Nevertheless the stability of the function was generally verified since asymptotic approximations are not exact.

2. One-step truncation error, $e_{t,n}$: To study $e_{t,n}$ the 1620 analysis for total truncation error was again used. Since $e_{t,1}$, the one-step error made during the first step, is generated by the accumulated error

function, the analysis necessarily contained the rudiments of a one-step error function. The only modification necessary to generate these one-step errors continuously was to make the computer "think" that each step was the first. This technique was applied to the integration of many differential equations having closed form solutions and was found to be extremely accurate. Although the level of effort did not permit extensive application of this technique to the thermal equation, the runs that were made indicated that any practical step-size gave an $e_{t,n}$ of less than 0.05°R.

Since the sum of the accumulated errors is bounded by ϵ, Eq. (35) can be written as

$$E_n = e_{t,n} + \epsilon \tag{36}$$

The results of the error analysis indicate that $e_{t,n} < 0.05°R$ and $\epsilon < 0.1°R$; therefore, the total error attributable to the numerical integration is

$$E_n < 0.15°R \tag{37}$$

which is negligible considering the accuracy of the input data.

C. Integration Technique When Function is Nondifferentiable

A major contribution of the numerical analysis investigation was the discovery and elimination of a significant error that was due to misapplication of the integration techniques employed in some previous similar studies. All standard numerical techniques assume that the function to be integrated is continuously differentiable at every point in the integration interval. This is not true of the thermal equation due to the behavior of the constant, C_1. When the orbiting vehicle enters or leaves the planet's shadow, C_1 may suddenly change from a relatively large number to almost zero or vice versa, causing the function to be nondifferentiable at the sun-shade points. The 1620 analysis revealed that the single-step error in an interval containing a sun-shade point was much larger (up to 10°R larger) than the total accumulated error just prior to that interval. In support of the stability conjecture, even this very large error became negligible after only a few integration steps.

This difficulty is completely eliminated by subdividing each interval containing a sun-shade point so that the nondifferentiable point coincides with the interval's boundary and thus does not exist within the interval.

V. DIGITAL COMPUTER PROGRAM

The determination of impinging heat loads and transient temperatures of up to 200 surface elements of a spacecraft in orbit is an ideal application of a high-speed digital computer. Performing this work in any other manner would be impractical at best. Accordingly, an IBM 7094 computer program incorporating the theory and numerical techniques described in Sections II, III, and IV has been written and checked out.

Programming was done in FORTRAN to facilitate any modifications that the program users may wish to perform. The program evolved by writing intermediate versions and debugging each only until the subsequent version became operable. In this way it was possible to test minor changes and corrections while extensive modifications were still being developed on paper. To avoid recompiling the entire source deck when incorporating changes, the program was organized as a pilot routine with a number of basic subroutines.

A User's Manual supplementing this final report gives a description of all subroutines, includes a table of planetary constants, and explains data preparation and output interpretation. The following section is intended only to introduce the program and to summarize some of its capabilities and applications. Further information can be obtained from the User's Manual.

A. Summary of Program Capabilities and Applications

The computer program is designed to compute and print out impinging heat fluxes and/or temperatures of a vehicle in orbit about the moon or any of the planets excepting Pluto. The orbiting craft may be spinning or may have a fixed orientation with respect to either the sun or the body it orbits. The planet's surface temperature, which is used in determining the amount of impinging thermal radiation originating from the planet, may be assumed to be constant or variable.[a]

---

a/ If the planet has a significant atmosphere, the surface temperatures tend to approach an average value. Further, the presence of an atmosphere, which may change considerably from one orbit to the next, makes it difficult to prepare representative albedo input data. Therefore, the method for constant (i.e., average) planet temperatures is recommended for most planets. The variable planet temperature method is only applicable to celestial bodies like the moon.

The program will determine heat loads during one orbit or any fraction thereof. When temperatures are required, more than one orbit may be specified. However, if all of the temperatures become stable (i.e., they differ by less than 0.5°R from one orbit to the next), the case is automatically terminated.

Emissivity, specific heat, and density of the vehicle substrate(s) and coating(s) are temperature-dependent. A standard NASA format for specifying material properties is employed. Up to 21 pairs of material property versus temperature from 0° to 10000°R (the sun's effective temperature) may be specified. Absorptivity with respect to heat flux radiated by the planet is found as a function of the effective temperature of that part of the planet actually "seen" by the orbiting object (see p. 30). A maximum of eight tables of emissivity may be used. Eight tables each of specific heat and density may also be used corresponding to eight possible substrate materials for the vehicle skin.

When temperature calculations are desired, up to eight different schedules of internal heat versus time can be used. Each set of data is read in as a table of internal heat and the switching time corresponding to a change to the next value of internal heat. As many as 20 different values (10 duty cycles) may be included in each of the eight tables. If the program runs for more than one orbit, the same sequence of internal heat loads is applied for successive orbits.

Satellite position in orbit is given by the true anomaly, ϕ , measured from perigee. A starting value, ϕ_o , and a step-size, $\Delta\phi$, are read in. ϕ_o must be between 0° and 360° and $\Delta\phi$ must be a submultiple of 360°. For example, 5°, 6°, 7.5°, 8°, 9°, or 10° are all acceptable values for $\Delta\phi$ but 7° is not since 360/7 is not an integer.

The program may internally subdivide $\Delta\phi$ to give the "optimum" interval with respect to accuracy and computer time; however, the input value of $\Delta\phi$ will not be exceeded. For temperature calculations, external heat fluxes are considered constant throughout the specified $\Delta\phi$ interval provided the vehicle does not pass in or out of the planetary shadow during the time corresponding to $\Delta\phi$. Furthermore, only one change in internal heat for each element is recognized per interval. MRI's experience indicates (at this time) that $\Delta\phi = 10°$ is a reasonable upper bound.

The sun's position relative to the orbit may be given conventionally, as right ascension and declination, which can be obtained from an ephemeris, or the sun's position may be specified in terms of angles, α , γ , β , relative to X_p , Y_p , Z_p coordinate axes.

As many as 200 elements of oriented vehicles may be processed in a single case. Each of these elements has its own thickness, initial temperature, and position on the satellite sphere. However, coating and substrate materials as well as internal heat duty cycles are restricted to eight choices of each as previously noted.

Effects of variations of thickness, initial temperature, material or internal heat loads can be studied in a single case if a number of elements are chosen with the same position but with different values for the other parameters. Thus a single case may be an entire parametric study in itself. Additional flexibility is provided so that if any of the input parameters are to remain the same from one case to another, these unchanged values can be represented by blank fields in the input deck.

B. Assumptions

In order to write a practical program to fulfill the project's objectives, it was necessary to introduce certain simplifying assumptions. These assumptions, none of which appreciably affects the program's accuracy or usefulness, are summarized in part below:

1. Conduction and convection between the vehicle and its surroundings are neglected. This assumption is valid for orbits about the moon and is reasonable for missions about other planets since orbits are usually well above any significant atmosphere to minimize drag.

2. Perturbations are neglected. This assumption is acceptable unless orbital missions of very long duration are to be analyzed. In these cases the program could be modified to account for significant variations.

3. The sun's position with respect to the orbit is fixed. This assumption is reasonable unless the flight duration becomes an appreciable per cent of the planet's period. In this event, the mission can be subdivided and run as several cases, each case having the appropriate coordinates of the sun specified.

4. The solar constant is independent of the vehicle's orbital position. Since the semimajor axis of the vehicle orbit is small compared to the planet's distance from the sun, solar radiation is essentially constant throughout a given orbit.

5. Planet data, such as albedo and mass, are internally stored and therefore are assumed to be invariable (unless the program is modified). While these properties are essentially constant, the accepted values are occasionally refined. If the program's data are to be refined accordingly, part of the program must be changed and recompiled. This disadvantage is more than offset by the convenience of not having to include planet properties in the input data each time a case is to be run.

6. The planet's shadow is assumed to be cylindrically shaped and penumbral effects are neglected. The resulting error in sun-shade point and heat load determinations are negligible even for extremely large orbits.

7. All thermal radiation in this study is assumed to be diffuse. Except for the radiation emitted by a polished vehicle surface, this assumption is essentially correct. Since the vehicle radiates to space, it does not matter whether its surface emits specular or diffusely (i.e., the magnitude is important but the direction is not).

8. The albedo of a planet is assumed to be independent of surface position or features. An average value is used only because the local values depend on such variables as clouds and other atmospheric conditions which are difficult, if not impossible, to predict even on earth.

9. Internally generated heat is assumed to be uniformly distributed over the applicable vehicle surface. If this is not reasonable, the internal heat and corresponding surface element should be subdivided until the assumption is acceptable.

10. Planets are assumed to emit as smooth spheres. There is evidence[5] that topographical features of the moon's surface do significantly affect the way in which it radiates; however, additional investigations are required before surface effects can be accounted for in a program such as this.

11. The temperature of the dark side of a variable temperature planet, T_m , is assumed to be constant. This assumption is valid. For example, the heat flux radiated from the moon's back side is less than 1 per cent of that radiated at the subsolar point; therefore, neglecting variations in T_m introduces negligible errors in q_{planet} .

12. The vehicle's absorptivity to reflected solar radiation is assumed to be the same as its absorptivity to direct solar radiation, α_s . The spectral characteristics of solar radiation is probably changed when it is reflected; however, it is believed that the change has little effect on α_s .

VI. TYPICAL TEST CASES

Hundreds of test cases were run in the course of developing and debugging the computer program. Most of these runs were hypothetical cases designed to check out a specific subroutine or program function.

Although design, orbital, and thermal data on actual satellites have been rather vaguely reported, sufficient information to simulate Vanguard and Explorer missions has been obtained. Results of these two runs will be summarized and a more informative lunar mission will be described in the following sections.

A Lunar Excursion Module Hypothetical Mission

Data for the proposed Lunar Excursion Module (LEM) moon orbit were prepared and run. Fourteen surface elements painted either black or white were analyzed. LEM was planet-oriented; its altitude varied from 10 miles to 190 miles. The orbit parameters were such that perilune occurred over the intended landing sight, which was 13° south of the moon's equator and 3° east (as seen from earth) of the moon's prime meridian.

Pertinent orbit data were as follows:

$a = 6.230 \times 10^6$ ft.

$b = 6.212 \times 10^6$ ft.

$i = 13°$

$\Omega = 87°$

$\omega = 270°$

$\phi_o = 0°$

The mission was "flown" on December 1, 1963. The sun's position in selenographic coordinates as given by an ephemeris was

colongitude = 88.74°

declination = 0.86°

Therefore,

$$RA = \text{longitude} = 90° - \text{colongitude} = 1.26°$$

$$DEC = 0.86°$$

The temperature-time results of differently oriented and painted surface elements reveal several interesting characteristics.

In Fig. 12, a white element facing away from the moon initially cools even though it is "looking" almost directly at the sun. The temperature of a similarly oriented element, painted black, rises to a peak at about $\phi = 60°$ and then drops as it gradually turns away from the sun.

The temperature curves of black and white elements facing the moon (see Fig. 13) are similar to each other since black and white paint absorbs long wavelength radiation (the moon's in this case) almost equally. Just before entering the moon's shadow and just after leaving the shadows, these elements are briefly irradiated by the sun. This shows up as a hump in the black element's curve at about $\phi = 100°$ and $\phi = 260°$.

Comparison of the black elements on Figs. 12 and 13 reveals that at this low altitude, the "lunar constant" is almost as great as the solar constant. In fact the black element facing the moon absorbs considerably more heat than the white element facing the sun.

To learn the effect of not considering the moon's surface temperature gradients, a "constant temperature" case was run. The results, also plotted in Fig. 13, are "flat" curves that average out the maximum and minimum peaks of the "variable temperature" curves. The 100°R deviations are errors caused by neglecting the moon's temperature variations.

These results confirm the importance of the variable temperature planet method in analyzing lunar missions.

B. Vanguard and Explorer Earth Satellites

A Vanguard satellite placed in orbit February 17, 1959, was thermally analyzed on the computer. The following approximate orbital data were used:

$a = 27.27 \times 10^6$ ft.

$b = 26.90 \times 10^6$ ft.

$i = 33°$

$\Omega = 60°$

$\omega = 270°$

$RA = 329.0°$

$DEC = -12.3°$

Averages of α_v and α_s values obtained from G. Hass, who coated the sphere, and from M. Schach, who performed the thermal analysis of Vanguard, were used.[6,7]

The Vanguard temperature, which was internally sensed, stabilized after several days. The skin thickness of the simulated satellite was adjusted to give a similar time lag.

The predicted temperature history was similar to that of the actual Vanguard and the two curves stabilized within 4°R.

The Explorer I - 1958 Alpha was also simulated. The predicted maximum temperature was about 560°R and the minimum was approximately 410°R in the shade. The cyclic temperature-time curve closely followed that reported by Buwalda and Hibbs.[8]

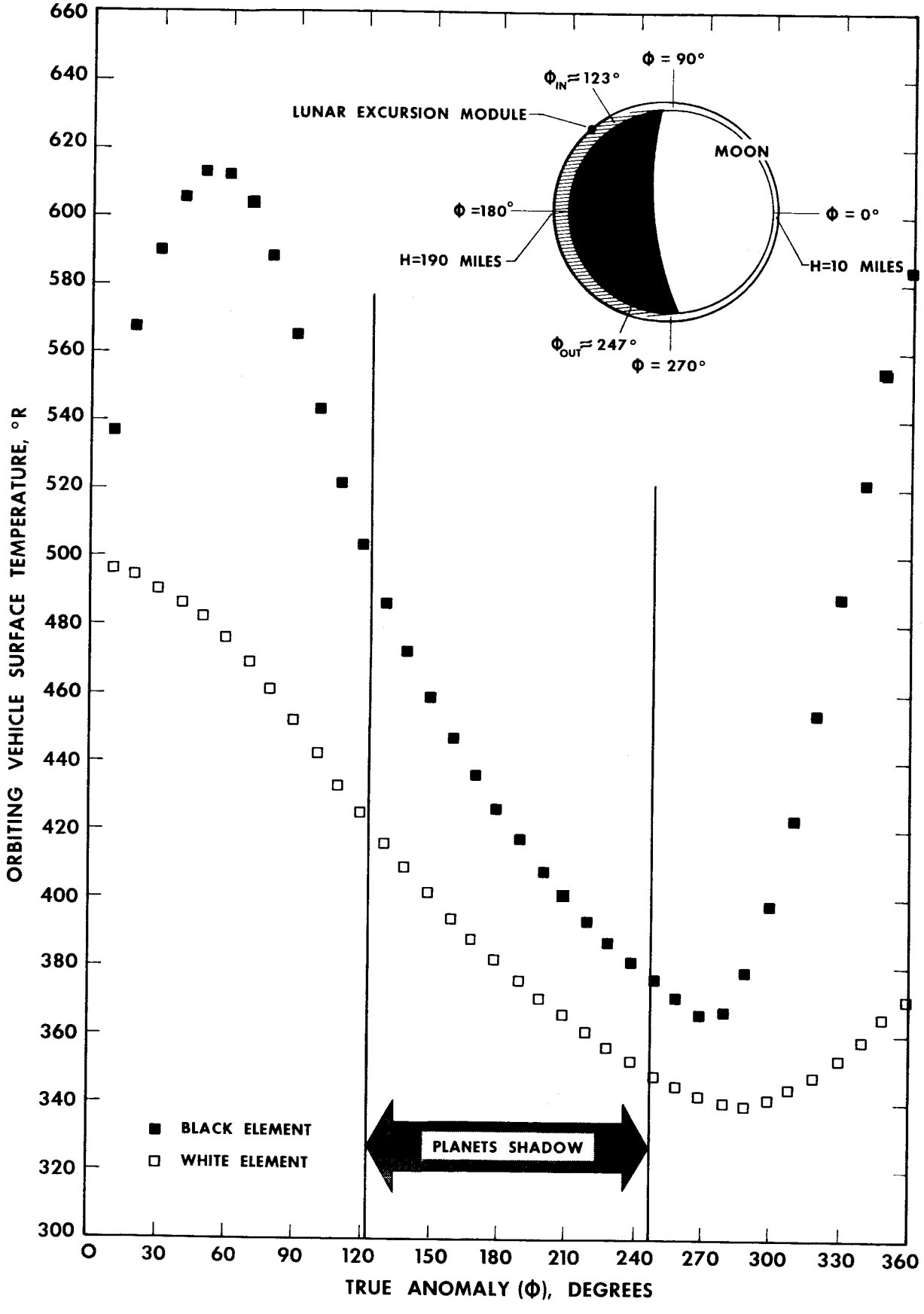

Fig. 12 - Simulated Lunar Excursion Module; Elements Face Away from the Moon

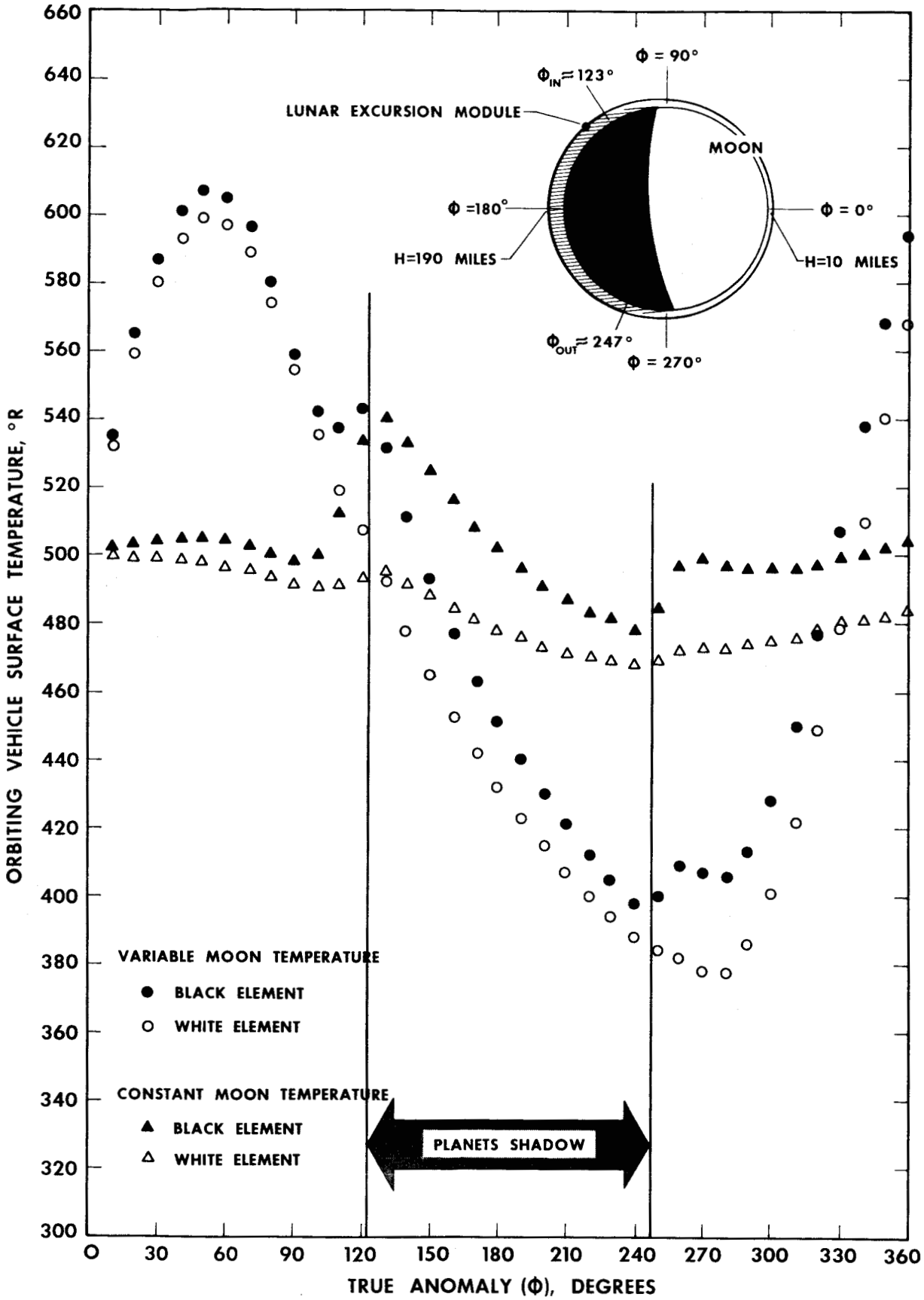

Fig. 13 - Simulated Lunar Excursion Module; Elements Face the Moon

VII. CONCLUSIONS AND RECOMMENDATIONS

An operational computer program to predict spacecraft heat loads and temperatures has been developed.

The program was not designed for any particular vehicle-mission combination, but rather it was developed to be applicable to all hypothetical and actual space projects. While there are no serious assumptions incorporated into the celestial, thermal, and numerical theory (see Section V-B), the level of effort was such that certain conditions could not be considered in the initial project without sacrificing the desired versatility.

The program was written so that it could be readily expanded to include additional features and details. Based on our knowledge of the program and of NASA MSC's objectives, we recommend that the following modifications be considered:

1. Include thermal conduction and radiation between vehicle surface elements. This expansion could probably incorporate programs developed by other organizations as subroutines.

2. Include the effects of shadows cast by part of the vehicle on itself. This modification could be so complicated that it might be necessary (economically) to perform this change re specific vehicle configurations, such as the Apollo Command Module, LEM, and space stations.

3. Modify the celestial mechanics theory to be applicable to earth-moon missions and interplanetarry operations.

4. Include the effects of the moon's topographical surface features on spacecraft heating if these effects prove to be significant.

5. Include the effects of perturbative forces. This modification is probably necessary for orbits of long duration.

6. Combine planet-oriented and sun-oriented options. This change would be applicable to planet-oriented vehicles that have solar panels facing the sun.

REFERENCES

1. Finch, Harold L., "An Analytical Study of Satellite Temperature Variations," ASD TR 61-394, Vol. 1, 1961.

2. Anon., "The American Ephemeris and Nautical Almanac," United States Government Printing Office, Published Annually.

3. Personal correspondence from Frank Kreith, Professor of Mechanical Engineering, University of Colorado, Oct. 15, 1963.

4. Henrici, Peter, "Discreet Variable Methods in Ordinary Differential Equations," John Wiley and Sons, 1962, pp. 83-84.

5. Niedz, F.J., "Survey of the Physical and Environmental Parameters of the Moon," NASw-410-20-13-10, Prepared for NASA Office of Manned Space Flight by General Electric under Contract NASw-410, Feb. 1963.

6. Personal correspondence from Alan Bradford (for Georg Hass), Chief, Evaporate Films Section, Physics Research Laboratory, U.S. Army Engineer Research and Development Laboratories, Fort Belvoir, Virginia, Dec. 23, 1963.

7. Personal correspondence from Milton Schach, Head, Thermal Systems Branch, NASA Goddard Space Flight Center, Dec. 24, 1963.

8. Buwalda, E.P., and Hibbs, A.R., "Satellite Temperature Measurements for 1958 Alpha-Explorer," External Publication No. 481, Jet Propulsion Laboratory, 1958.

9. Burrington, R.S., "Handbook of Mathematical Tables and Formulas," Handbook Publishers, Inc., 1956.

10. Seavey, Marden H., "The Temperature of an Object above the Earth's Atmosphere," AFCRC-TN-58-633, Geophysics Research Directorate, Air Force Cambridge Research Center, 1959.

11. Ballinger, J., et al., "Thermal Environment of Space," ERR-AN-016, Convair Astronautics Division, General Dynamics Corporation, Nov. 1960.

APPENDIX A

INTERSECTION OF ORBIT AND SHADOW

The intersection of the orbit and the shadow can be determined by simultaneously solving the equations that express the vehicle path and the shadow's trace on the orbital plane.

If $\beta = 0°$ or $\beta = 180°$, the trace of the shadow is a circle of radius r_p that does not intersect the vehicle orbit.

If $0° < \beta < 180°$ but $\beta \neq 90°$, the trace is a semiellipse as shown in Fig. A-1a. The equation of the orbit path, based on the notation shown in Fig. A-1b, is

$$\frac{(X_p+c)^2}{a^2} + \frac{Y_p^2}{b^2} = 1 \qquad \text{(A-1)}$$

The corresponding expression for the shadow's intersection with the orbital plane is

$$\frac{(X_p \cos \Sigma + Y_p \sin \Sigma)^2}{A^2} + \frac{(X_p \sin \Sigma - Y \cos \Sigma)^2}{B^2} = 1 \qquad \text{(A-2)}$$

Equations (A-1) and (A-2) combine to yield a biquadratic (quartic), which is solved in this study by the Ferrari method. Some numerical approaches may be faster, but become unstable in certain cases. The Ferrari method, which can be used to solve any quartic equation, is explained in most theory-of-equation texts and many mathematical handbooks (e.g., Burrington[9]).

The X_p coordinates having been found, the corresponding Y_p values can be determined from either Eq. (A-1) or from Eq. (A-2); however, care must be taken to avoid accepting an extraneous root. This potential source of difficulty is circumvented by solving both equations for Y_p^2 and equating the expressions. The result reduces to the function below which is single-valued for all X_p :

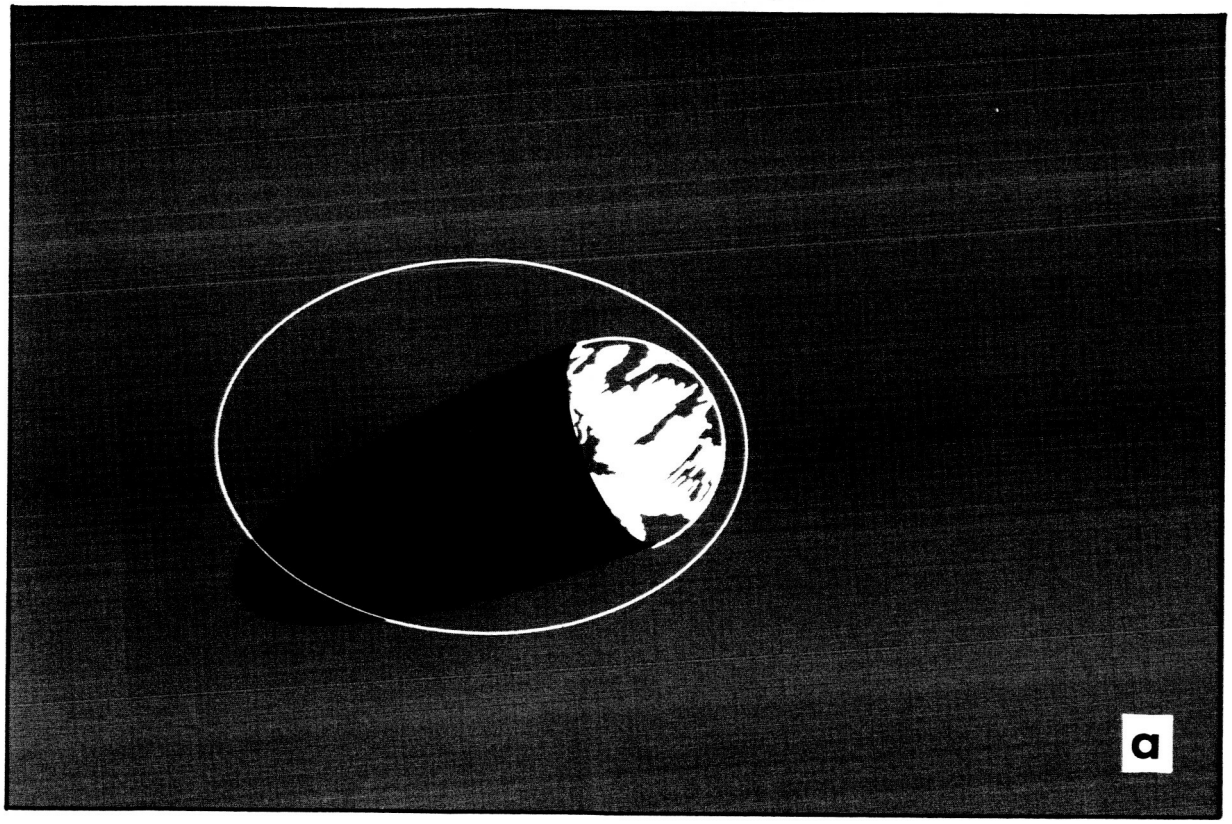

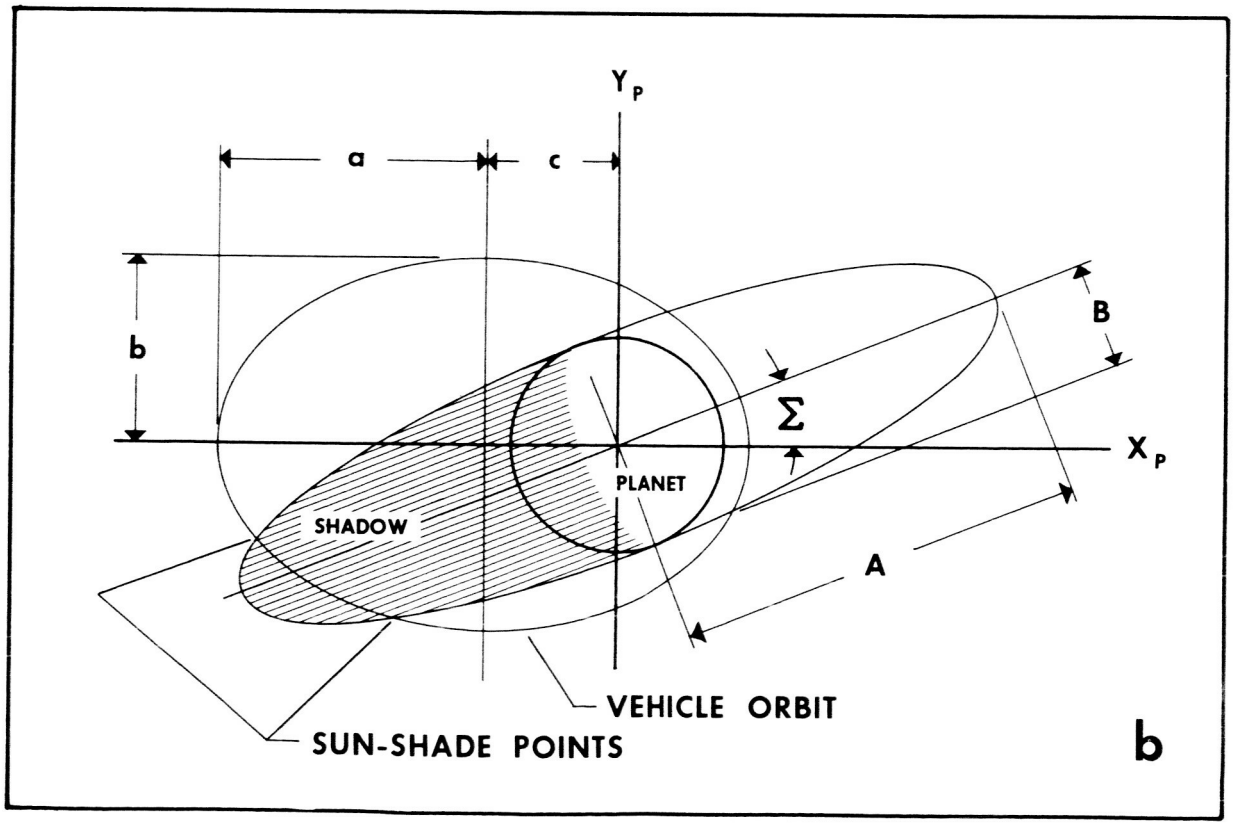

Fig. A-1 - Intersection of Planet's Shadow and Orbit Plane

$$\frac{Y_p}{a} = \chi \left[(\cos \beta \cos \Sigma)^2 + \sin^2 \Sigma\right] - \left(\frac{B}{a}\right)^2$$
$$+ \left(\frac{b}{a}\right)^2 \left[1 - \left(\chi + \frac{c}{a}\right)^2\right] \left[(\cos \beta \sin \Sigma)^2 + \cos^2 \Sigma\right] \tag{A-3}$$

where

$$\chi = \frac{X_p}{a} \tag{A-4}$$

The true anomaly of the sun-shade points is calculated from

$$\tan \phi = \frac{Y_p}{X_p} \tag{A-5}$$

If the shade and orbit ellipses do not intersect or if they cross in only two places, the quartic equation can yield spurious (i.e., false) real roots. Since Eq. (A-3) is valid only at the ellipse intersections, solutions of it corresponding to spurious roots are meaningless. Therefore, the validity of each pair of coordinates must be determined, and this is done by testing to see if the X_p , Y_p values satisfy both Eq. (A-1) and Eq. (A-2).

If $\beta = 90°$, the trace of the shadow ellipse degenerates to a pair of parallel lines which are expressed in polar form as

$$\rho \sin (\Sigma - \phi) = r_p \tag{A-6a}$$

$$\rho \sin (\Sigma - \phi) = - r_p \tag{A-6b}$$

where ρ is the distance from the lines to the planet's center of mass. A similar expression of the orbit ellipse is

$$\rho = \frac{b^2}{a + c \cos \phi} \tag{A-7}$$

Eliminating ρ from Eqs. (A-6a) and (A-7) gives

$$(b^2 \sin \Sigma - cr_p) \cos \phi - b^2 \cos \Sigma \sin \phi - ar_p = 0 \qquad \text{(A-8a)}$$

In general, Eq. (A-8a) is transformed to a quadratic in $\cos \phi$ by substituting $\pm (1 - \cos^2 \phi)^{\frac{1}{2}}$ for $\sin \phi$. The roots of this quadratic are put back into Eq. (A-8a) to give values for $\sin \phi$. Once $\sin \phi$ and $\cos \phi$ are known, ϕ is easily found. A similar procedure yields the other sun-shade point if ρ is eliminated between Eqs. (A-6b) and (A-7) giving

$$(b^2 \sin \Sigma + cr_p) \cos \phi - b^2 \cos \Sigma \sin \phi + ar_p = 0 \qquad \text{(A-8b)}$$

If the coefficient of $\sin \phi$ or $\cos \phi$ in Eq. (A-8) vanishes, the problem is less difficult in that $\sin \phi$ or $\cos \phi$ can be solved for directly and the corresponding function is determined from either $\sin \phi = \pm(1-\cos^2 \phi)^{\frac{1}{2}}$ or $\cos \phi = \pm(1 - \sin^2 \phi)^{\frac{1}{2}}$.

Equations (A-5) and (A-8) may give zero, two or four valid mathematical roots; however, two of these may not satisfy the condition that the sun-shade points lie on the shaded side of the orbit. A root is discarded unless the angle between the line connecting the sun-shade point and the planet and the line of the sun's projection on the orbital plane is obtuse.

APPENDIX B

RADIATION HEAT TRANSFER DERIVATIONS

A general expression for thermal radiation from one surface to another can be derived by considering the total radiation from the emitter. This may be visualized by placing a hemisphere over the emitting surface element A_e as shown in Fig. B-1. This hemisphere will intercept all of the heat emitted from A_e and the radiation "seen" by an element dA_r is given by the familiar "square of the distance" equation

$$dq = I \frac{\epsilon \cos \phi_e A_e \cos \phi_r}{D^2} dA_r \qquad \text{(B-1)}$$

where ϵ is the emissivity of A_e. The proportionality factor, I, is known as the intensity of radiation. Assuming that the emitting surface is diffuse, its intensity is independent of direction and is constant. The

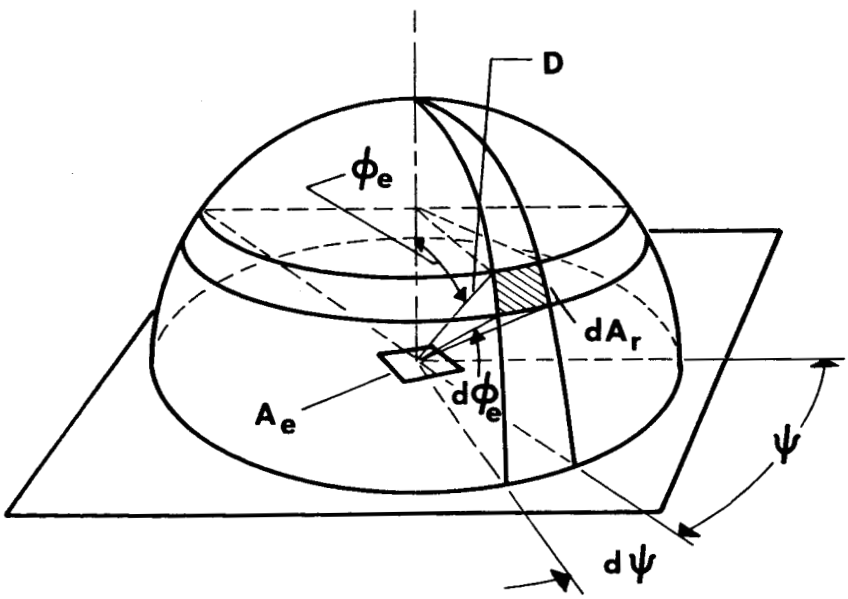

Fig. B-1 - Mathematical Model for Deriving General Thermal Radiation Equation

apparent or "intercepted" intensity is proportional to A_e as seen from dA_r on the hemisphere. Thus

$$I(\phi_e) = I \cos \phi_e \tag{B-2}$$

which is Lambert's cosine law. If dA_r is on the hemisphere surface, ϕ_r is 0°; therefore,

$$dq = \frac{I \cos \phi_e A_e \epsilon dA_r}{D^2} \tag{B-3}$$

Writing dA_r in terms of ϕ_e and ψ, Eq. (B-3) becomes

$$q = IA_e\epsilon \int_0^{2\pi} d\psi \int_0^{\pi/2} \cos \phi_e \sin \phi_e d\phi_e = IA_e\epsilon\pi \tag{B-4}$$

The heat radiated by A_e is

$$q_{out} = \epsilon(\sigma T_e^4)A_e = \epsilon EA_e \tag{B-5}$$

where E is the emissive power of A_e. Since all of the emitted heat is intercepted by the hemisphere, the heat emitted is equivalent to the heat received. Equating Eqs. (B-4) and (B-5), simplifying the results, and solving yields

$$I = \frac{E}{\pi} \tag{B-6}$$

Combining Eqs. (B-1) and (B-6) and introducing the absorptivity, α, of the receiving surface gives the general equation for radiant heat transfer between two surfaces

$$dq = \frac{E \cos \phi_e A_e \cos \phi_r \alpha\epsilon}{\pi D^2} dA_r \tag{B-7}$$

In the following sections, the general formula, Eq. (B-7), will be used to derive specific equations that express the amount of planetary and albedo heat that is "seen" and/or absorbed by a spinning or oriented vehicle. Derivations will be made for constant temperature planets as well as for variable temperature planets.

1. Planet heat flux, spinning vehicle, constant planet temperature: Seavey[10] simplified the mathematics by utilizing a theorem which states that the flux incident on a small surface element from an extended source of uniform brightness is independent of the two shapes. A modification of Seavey's solution is developed by first replacing the part of the planet that the satellite "sees" with a concave disk of radius ℓ as shown in Fig. B-2a. This geometrical substitution can be comprehended visually by observing that the sun, a uniform emitter with respect to surface position, appears to the observer on earth as a disk. Similarly, the satellite is replaced by a flat disk which has an infinitesimal area compared to the planet disk.

It can be seen in Fig. B-2b that every line between the satellite and the planet perpendicularly intersects D_p. Likewise, the satellite-planet lines can be made normal to D_v by letting D_v pivot about its center allowing the planet differential elements to "see" different orientations of the satellite disk. Thus, in Fig. B-2c, element A "sees" A' while element B "sees" B'. The "wobbling" of D_v is justified by the aforementioned theorem employed by Seavey.

Equation (B-7) is modified to express the heat received by satellite area, A_v, from a ring-shaped element of area, dA_p, as follows

$$dq_{planet} = \frac{E \cos \phi_p \cos \phi_v A_v \epsilon_p \alpha_p}{\pi \ell^2} dA_p \qquad \text{(B-8)}$$

Assuming that celestial bodies are perfect emitters (i.e., $\epsilon_p = 1$) and substituting $\phi_p = \phi_v = 0°$, Eq. (B-8) reduces to

$$dq_{planet} = \frac{EA_v \alpha_p}{\pi \ell^2} dA_p \qquad \text{(B-9)}$$

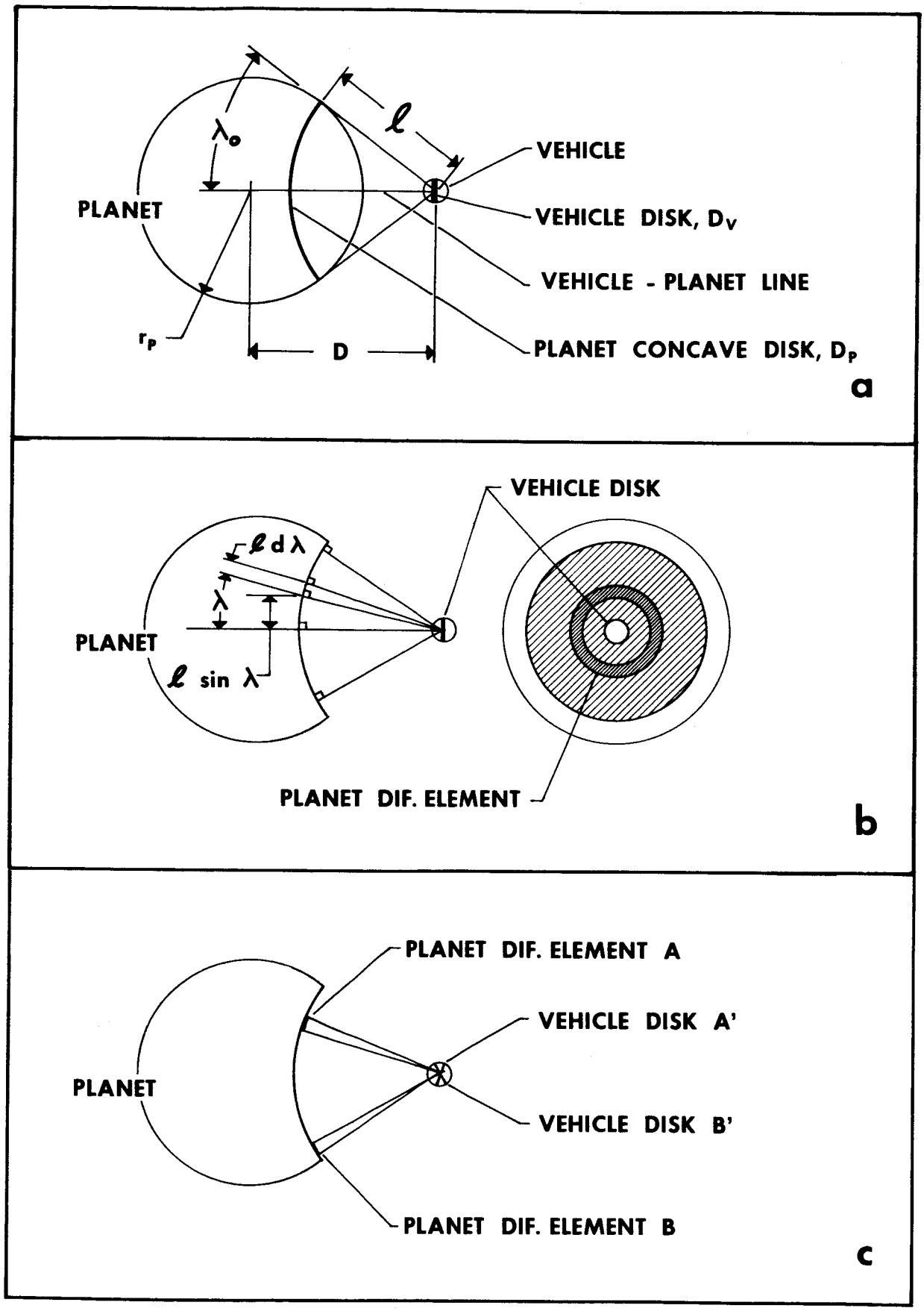

Fig. B-2 - Seavey's Model for Determining Radiation between Two Spheres of Uniform Brightness

The planet differential area and the effective vehicle area are

$$dA_p = \left[2\pi(\ell \sin \lambda)\right]\left[\ell \, d\lambda\right] = 2\pi\ell^2 \sin \lambda \, d\lambda \tag{B-10}$$

and

$$A_v = \pi r_v^2 \tag{B-11}$$

The emissive power is

$$E = \sigma T_p^4 \tag{B-12}$$

where T_p is the average planet temperature. A heat balance on the planet yields

$$T_p = \left[\frac{S(1-R)}{4\sigma}\right]^{\frac{1}{4}} \tag{B-13}$$

Combining Eqs. (B-12) and (B-13) gives

$$E = \sigma \left\{\left[\frac{S(1-R)}{4\sigma}\right]^{\frac{1}{4}}\right\}^4 \tag{B-14}$$

which becomes

$$E = \frac{S(1-R)}{4} \tag{B-15}$$

Substituting Eqs. (B-10), (B-11), and (B-15) into Eq. (B-9) and integrating yields the desired relationships

$$q_{planet} = 2S(1-R)\alpha_p F_1 \pi r_v^2 \ , \ T_p = C \tag{B-16a}$$

$$\frac{q_{planet}}{4\pi r_v^2} = \frac{S(1-R)\alpha_p F_1}{2} \ , \ T_p = C \tag{B-16b}$$

where

$$F_1 = \frac{1 - \left[1 - \left(\frac{r_p}{D}\right)^2\right]^{\frac{1}{2}}}{\cancel{8}\ 4} \tag{B-16c}$$

The planet heat rate per unit area impinging on the spherical vehicle is

$$\frac{q_{planet}}{A_v} = 2S(1-R)F_1 \ , \ T_p = C \tag{B-16d}$$

A derivation not based on Seavey's theorem can also be made and will be presented in condensed form. The heat emitted from planet element dA_p (see Fig. B-3) and absorbed by a satellite of radius r_v is

$$dq_{planet} = \frac{E \cos \phi_p \cos \phi_v dA_p \alpha_p \epsilon_p \pi r_v^2}{\pi \rho^2} \tag{B-17}$$

Again substituting $\epsilon_p = 1$, $\phi_v = 0$, and $E = S(1-R)/4$ and integrating, Eq. (B-17) becomes

$$q_{planet} = \frac{S(1-R)r_v^2 \alpha_p}{4} \iint \frac{\cos \phi_p}{\rho^2} \cdot dA_p \tag{B-18}$$

It can be shown that

$$\cos \phi_p = \frac{D \cos \theta - r_p}{\rho} \tag{B-19}$$

$$\rho^2 = r_p^2 + D^2 - 2r_pD \cos \theta \tag{B-20}$$

and

$$dA_p = r_p^2 \sin \theta \, d\theta \, d\phi \tag{B-21}$$

where the variables are illustrated in Fig. B-3. Ballinger[11] used these three relations to evaluate an expression similar to Eq. (B-18), and from his work the following equality can be developed

$$\int\int \frac{\cos \phi_p}{\rho^2} \cdot dA_p = 2\pi \left\{ 1 - \left[1 - \left(\frac{r_p}{D} \right) \right]^2 \right\}^{\frac{1}{2}} \tag{B-22}$$

Combining the above expression with Eq. (B-18) gives

$$q_{planet} = \frac{S(1-R)\alpha_p}{\cancel{4}\,2} \left\{ 1 - \left[1 - \left(\frac{r_p}{D} \right)^2 \right]^{\frac{1}{2}} \right\} \pi r_v^2 \, , \; T_p = C \tag{B-23}$$

which is equivalent to Eq. (B-16).

2. Planet heat flux, spinning vehicle, variable planet temperature: The expression, Eq. (B-17), for radiant heat exchange between a surface differential element and a spherical satellite is applicable also to planets of variable temperature. If the planet has a negligible atmosphere and is a good thermal insulator, the element dA_p is in thermal equilibrium;[a] therefore, the heat emitted is equivalent to the solar heat absorbed as shown in Fig. B-4 and

---

a/ If mechanisms for heat transfer do exist (e.g., conduction and convection in a planet's atmosphere) so that dA_p is not in equilibrium, the surface temperatures tend to approach an average value. Further, the presence of an atmosphere, which may change considerably from one orbit to the next, makes it impractical if not impossible to prepare meaningful albedo input data. Thus, average albedo values are used for most planets and the method for constant (i.e., average) planet temperatures should be employed. Consequently, the method of variable temperatures is applicable only to bodies such as the moon.

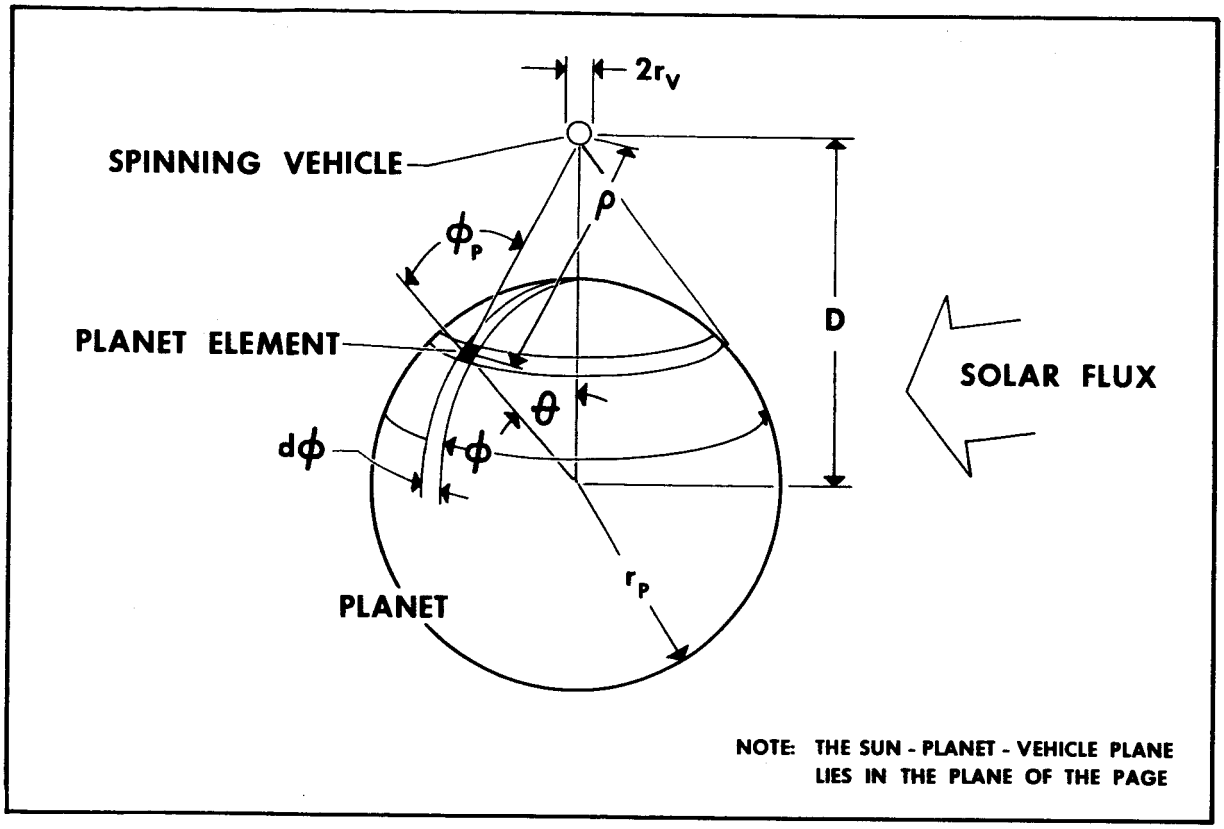

Fig. B-3 - Geometry for Determining Heat Exchange between Planet and Spinning Vehicle

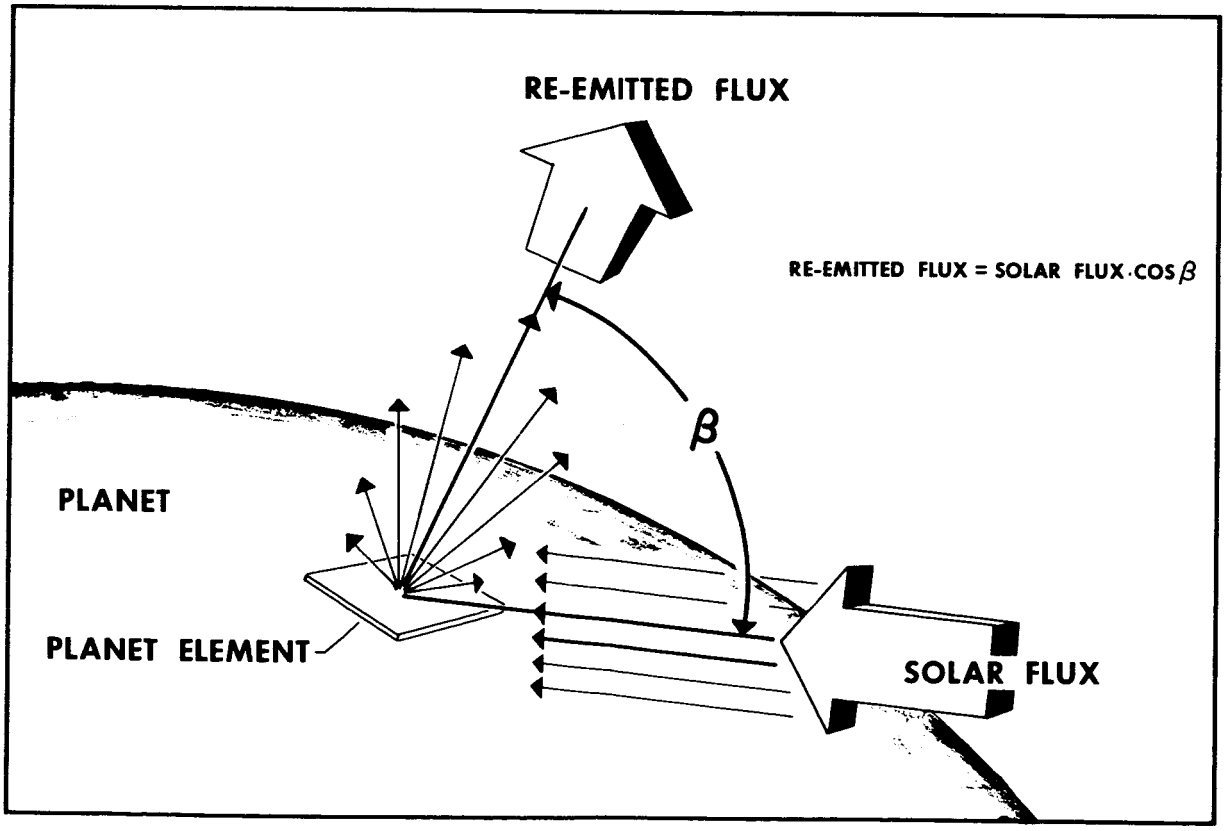

Fig. B-4 - Heat Emitted by an Element of a Variable Temperature Planet

$$E = q_{in} = q_{out} = S(1-R) \cos \beta \tag{B-24}$$

Combining Eqs. (B-17) and (B-24), letting $\epsilon_p = 1$ and $\phi_v = 0$, integrating and rearranging yields

$$q_{planet} = 4 \left[\frac{S(1-R)r^2 \alpha_p}{4} \right] \iint (\cos \beta) \left(\frac{\cos \phi_p}{\rho^2} \cdot dA_p \right) \tag{B-25}$$

The function $\cos \beta$ can be shown to be

$$\cos \beta = \cos \theta \cos \theta_s + \sin \theta \sin \theta_s \cos \phi \tag{B-26}$$

which can be approximated by

$$\cos \beta \approx \cos \theta_s \tag{B-27}$$

Equation (B-27) can be mathematically substantiated for small values of θ since

$$\lim_{\theta \to 0} \cos \beta = \cos \theta_s \tag{B-28}$$

For larger values of θ, the altitude is large and F is small; consequently, the error introduced by the approximation is relatively insignificant. Combining Eqs. (B-25) and (B-27) gives

$$q_{planet} \approx 4 \cos \theta_s \left[\frac{S(1-R)r^2 \alpha_p}{4} \iint \frac{\cos \phi_p}{\rho^2} dA_p \right] \tag{B-29}$$

Combining Eq. (B-22) and Eq. (B-29) gives

$$q_{planet} = 8S(1-R)\alpha_p F_2 \pi r^2 \ , \ T_p \neq C \tag{B-30a}$$

$$\frac{q_{planet}}{4\pi r_v^2} = 2S(1-R)\alpha_p F_2 \ , \ T_p \neq C \tag{B-30b}$$

where

$$F_2 \approx \left\{ \frac{1 - \left[1 - \left(\frac{r_p}{D}\right)^2\right]^{\frac{1}{2}}}{\cancel{8}\ 4} \right\} \cos\theta_s \tag{B-30c}$$

The variable temperature planet heat rate per unit area impinging on the spherical vehicle is

$$\frac{q_{planet}}{A_v} = 8S(1-R)F_2 \ , \ T_p \neq C \tag{B-30d}$$

An expression similar to Eq. (B-25) has been evaluated by Ballinger numerically on a digital computer. The resulting F factors[a] were tabulated as a function of altitude, H , and the sun-planet-satellite angle, θ_s . The approximate configuration factor, F_2 , is related to the tabulated factor $F(H,\theta_s)$ by

$$F_2 \approx \frac{F(H,\theta_s)}{\cancel{16}\ 8} \tag{B-31}$$

a/ The table of F values was duplicated at MRI as part of a study to determine the effect of surface topology on planet thermal emission.

Random values of $F(H,\theta_s)/16$ and the approximate function F_2 are plotted in Fig. B-5. As expected the per cent deviation is small for large values of F and the magnitude of deviation is negligible for low values of F, therefore, the approximation $\cos\beta \approx \cos\theta_s$ introduces insignificant errors into the derivation of F_2. Consequently, the F_2 function has been incorporated into the computer program in lieu of the slower table look-up method to find $F(H,\theta_s)/16$.

The dark side of a variable temperature planet is essentially in thermal equilibrium; therefore, the heat emitted can be derived from the relations that are applicable to a constant temperature planet.

The emissive power is

$$E = \sigma T_m^4 \tag{B-32}$$

where T_m is the dark side or minimum temperature of the planet. Combining Eqs. (B-32), (B-9), (B-10) and (B-11) and integrating gives

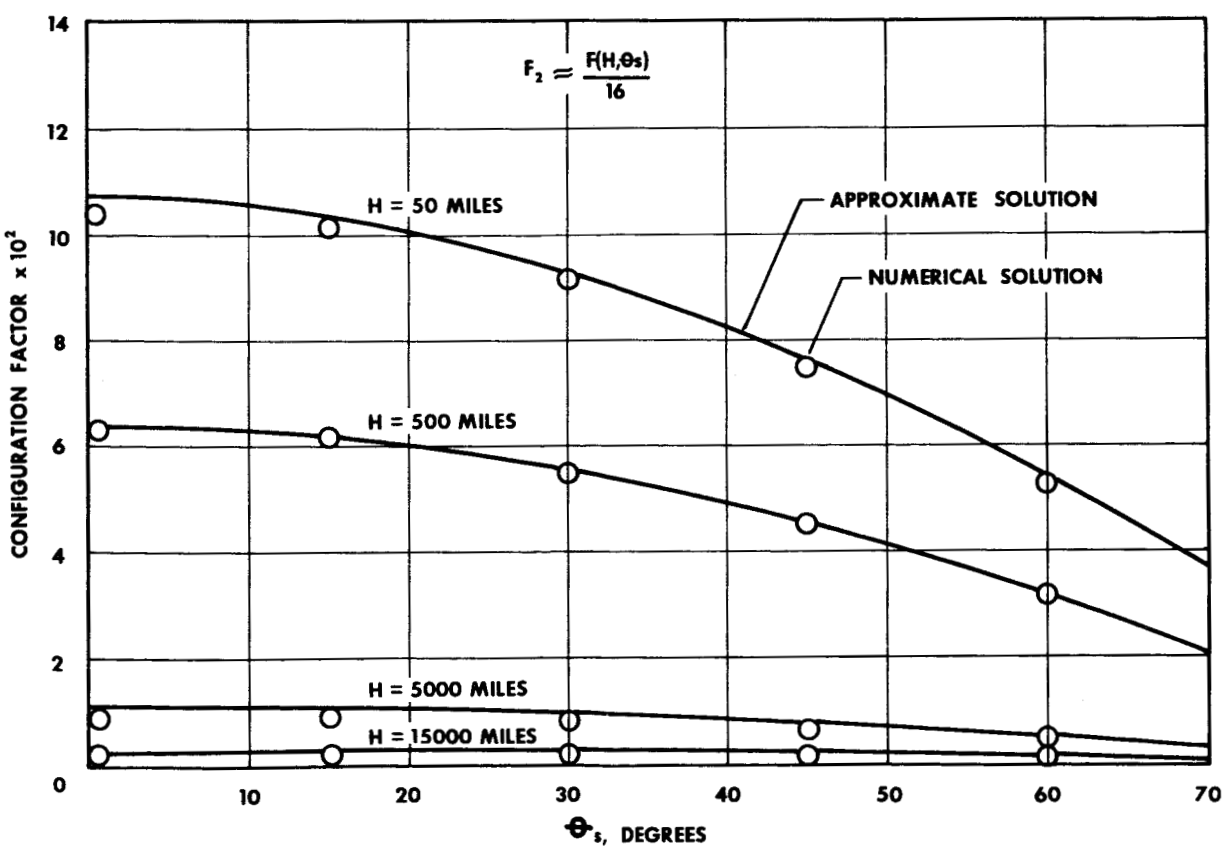

Fig. B-5 - Configuration Factors: Approximate and Numerical Solutions Compared

$$q_{planet} = 8\sigma T_m^4 \alpha_p F_1 \pi r_v^2 \ , \ T_p \neq C \text{ (dark side of planet)} \tag{B-33a}$$

$$\frac{q_{planet}}{4\pi r_v^2} = 2\sigma T_m^4 \alpha_p F_1 \ , \ T_p \neq C \text{ (dark side of planet)} \tag{B-33b}$$

where

$$F_1 = \frac{1 - \left[1 - \left(\frac{r_p}{D}\right)^2\right]^{\frac{1}{2}}}{\cancel{8}\,4} \tag{B-33c}$$

The heat impinging on the sphere is

$$\frac{q_{planet}}{A_v} = 8\sigma T_m^4 F_1 \ , \ T_p \neq C \text{ (dark side of planet)} \tag{B-33d}$$

3. Albedo heat flux, spinning vehicle: Solar radiation reflects diffusely from celestial bodies; therefore, the equations derived to express planetary diffuse thermal emission can be modified to be applicable to albedo calculations. The heat reflected from differential element dA_p a/(see Fig. B-3) and absorbed by A_v is given by the familiar relationship

$$dq_{albedo} = \frac{E \cos \phi_p dA_p \alpha_s \epsilon_s \pi r_v^2}{\pi \rho^2} \tag{B-34}$$

where E is the element's effective emissive power

$$E = SR \cos \beta \tag{B-35}$$

Combining Eqs. (B-34) and (B-35), letting $\epsilon_s = 1$, simplifying, and integrating gives

a/ Albedo includes solar energy bounced or scattered from the atmosphere above dA_p as well as that reflected from the planet surface element.

$$q_{albedo} = SR\ r_v^2 \alpha_s \iint (\cos\beta)\left(\frac{\cos\phi_p}{\rho^2} \cdot dA_p\right) \tag{B-36}$$

Introducing the approximation $\cos\beta \approx \cos\theta_s$ (see discussion preceding Eq.(B-29)),Eq. (B-36) becomes

$$q_{albedo} = SR\ r_v^2 \alpha_s \cos\theta_s \iint \frac{\cos\phi_p}{\rho^2}\, dA_p \tag{B-37}$$

The above integral term was evaluated in Eq. (B-22). Substituting Eq. (B-22) into Eq. (B-37) gives

$$q_{albedo} = 8\ SR\ \alpha_s F_2 \pi r_v^2 \tag{B-38a}$$

$$\frac{q}{4\pi r_v^2} = 2\ SR\ \alpha_s F_2 \tag{B-38b}$$

where

$$F_2 \approx \left\{\frac{1 - \left[1 - \left(\frac{r_p}{D}\right)^2\right]^{\frac{1}{2}}}{\cancel{8}\ 4}\right\}\cos\theta_s \tag{B-38c}$$

The albedo heat rate per unit area impinging on the spherical vehicle is

$$\frac{q_{albedo}}{A_v} = 8\ SR\ F_2 \tag{B-38d}$$

4. Planet heat flux, oriented vehicle, variable planet temperature: Equations that express the amount of thermal radiation received by a flat element in space can be developed from the general relationship, Eq. (B-7). The derivations are similar to those for a sphere; however, the plate is not necessarily symmetrical with respect to the satellite-planet line and, consequently, its orientation is relatively difficult to define. The heat absorbed by the flat plate element shown in Fig. B-6 from a planet of variable surface temperature is

$$dq_{planet} = \frac{E \cos \phi_p \cos \phi_v dA_p \alpha_p \epsilon_p A_v}{\pi \rho^2} \tag{B-39}$$

Substituting $\epsilon_p = 1$ and $E = S(1-R) \cos \beta$ (see Eq. (B-13)) into the above equation and integrating yields

$$q_{planet} = S(1-R)\alpha_p A_v \iint \frac{\cos \beta \cos \phi_p \cos \phi_v}{\pi \rho^2} dA_p \tag{B-40}$$

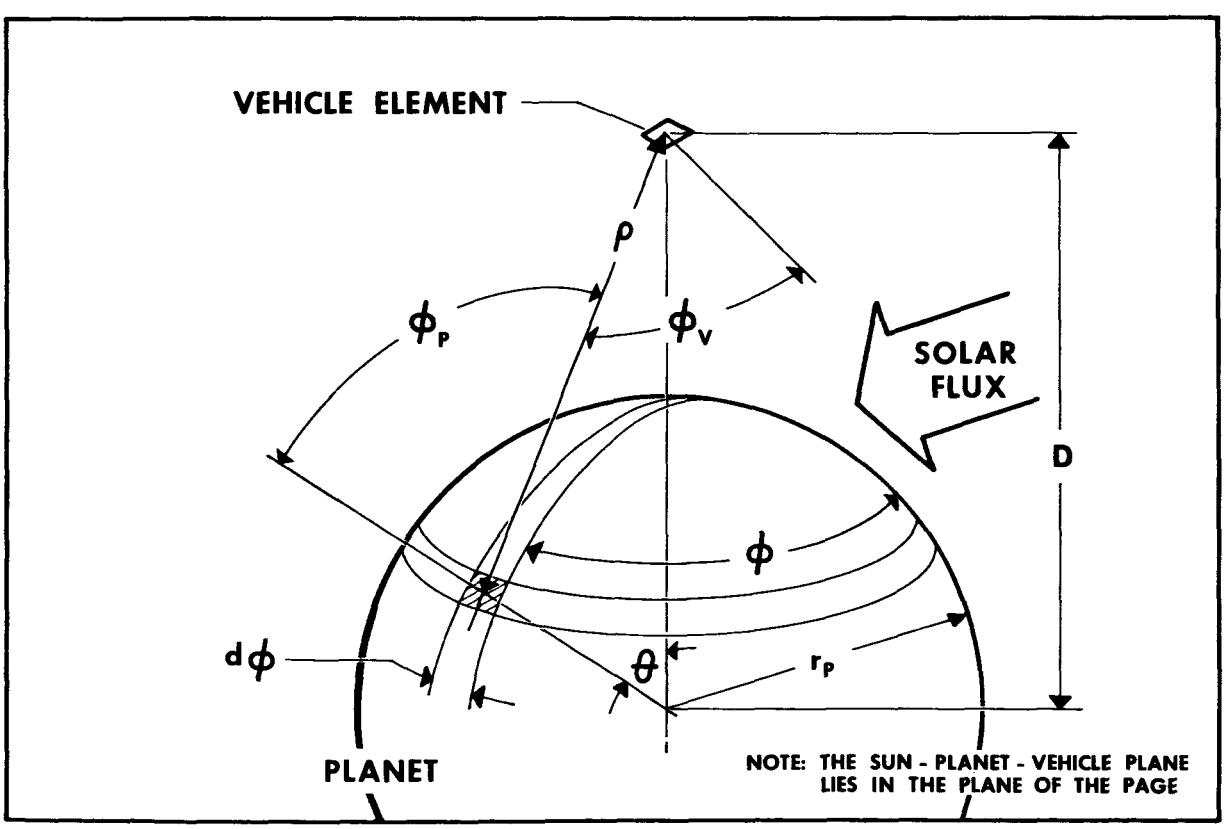

Fig. B-6 - Geometry for Determining Heat between Planet and Vehicle Element

Ballinger numerically integrated an equation similar to that above and from his work the following equality was developed

$$\iint \frac{\cos \beta \cos \phi_p \cos \phi_v}{\pi \rho^2} dA_p = F_3(H, \theta_s, \phi_c, \epsilon) \qquad \text{(B-41)}$$

where H is vehicle altitude and the parameters θ_s, ϕ_c, and ϵ are illustrated in Fig. B-7. Values of F_3 as a function of the four independent variables have been calculated and tabulated. The validity of the table was investigated and established by hand calculations for numerous special cases and for two general cases. Further, a check with Convair Astrodynamics and North American Aviation personnel who had, respectively, developed and used the data revealed no irregularities. Combining Eqs. (B-40) and (B-41) gives

$$q_{planet} = S(1-R)\alpha_p F_3 A_v \ , \ T_p \neq C \qquad \text{(B-42a)}$$

$$\frac{q_{planet}}{A_v} = S(1-R)\alpha_p F_3 \ , \ T_p \neq C \qquad \text{(B-42b)}$$

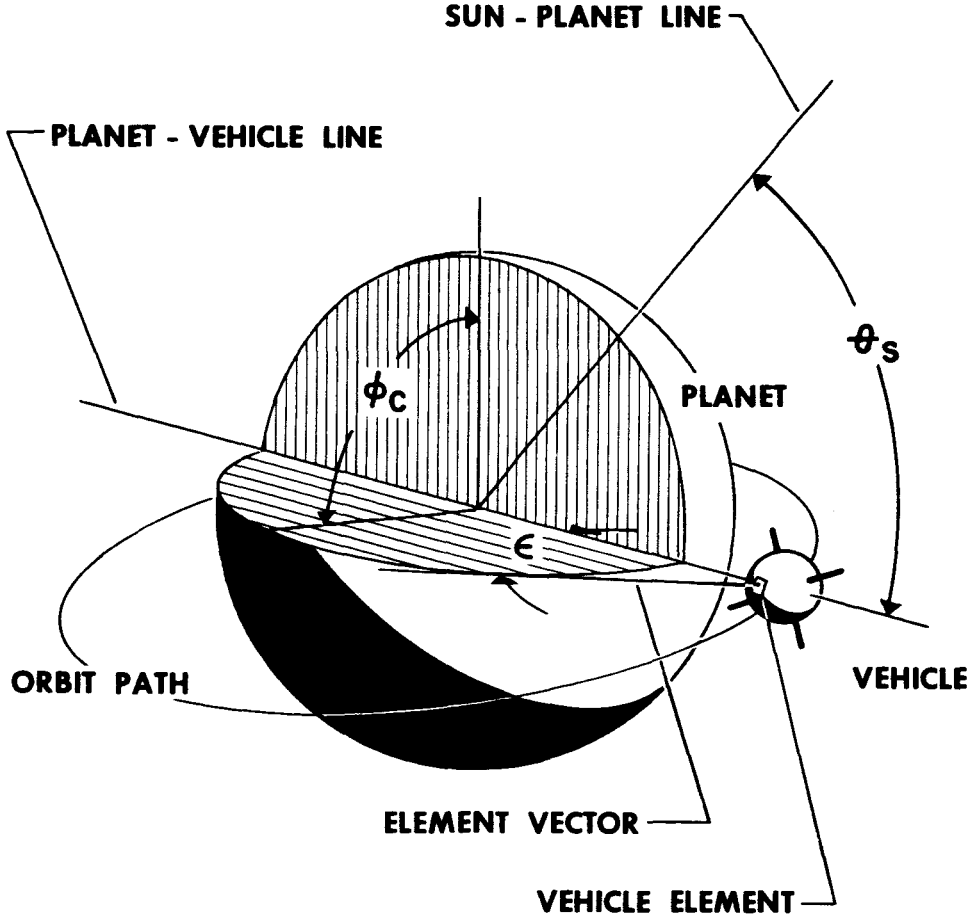

Fig. B-7 - Angular Variables for Determining Configuration Factors of Oriented Vehicles

where values of F_3 are found by table look-up. The planet heat rate per unit area impinging on the flat plate is

$$\frac{q_{planet}}{A_v} = S(1-R)F_3 \ , \ T_p \neq C \tag{B-42c}$$

5. Planet heat flux, oriented vehicle, constant planet temperature: The emissive power of a planet of uniform temperature is independent of β : $E = S(1-R)/4$ as given in Eq. (B-31). Substituting this expression for E into Eq. (B-39) and integrating gives

$$q_{planet} = \frac{S(1-R)\alpha_p A_v}{4} \iint \frac{\cos \phi_p \cos \phi_v}{\pi\rho^2} dA_p \tag{B-43}$$

Comparing Eqs. (B-41) and (B-43) it can be seen that

$$\iint \frac{\cos \phi_p \cos \phi_v}{\pi\rho^2} dA_p = \iint \frac{\cos (\beta=0) \cos \phi_p \cos \phi_v}{\pi\rho^2} dA_p \tag{B-44}$$

Introducing the approximation that $\cos \beta \approx \cos \theta_s$, which was previously shown to have a negligible effect on accuracy, the integral becomes

$$\iint \frac{\cos \phi_p \cos \phi_v}{\pi\rho^2} dA_p \approx F_3(H, \theta_s=0, \phi_c, \epsilon) \tag{B-45}$$

Combining Eqs. (B-45) and (B-43) gives

$$q_{planet} = \frac{S(1-R)\alpha_p F_4 A_v}{4} \ , \ T_p = C \tag{B-46a}$$

$$\frac{q_{planet}}{A_v} = \frac{S(1-R)\alpha_p F_4}{4} \ , \ T_p = C \tag{B-46b}$$

where values of F_4 are found by table look-up and are the same as F_3 except one of the independent variables is treated as a constant: $\theta_s = 0$. The impinging heat rate is

$$\frac{q_{planet}}{A_v} = \frac{S(1-R)F_4}{4} , \quad T_p = C \tag{B-46c}$$

The dark side of a variable temperature planet is essentially in thermal equilibrium; therefore, the heat emitted can be derived from the equations that are applicable to a planet of uniform temperature.

Substituting the emissive power ($E = \sigma T_m^4$) of the element shown in Fig. B-6 into Eq. (B-39), integrating, and introducing the equality given in Eq. (B-45) gives

$$q_{planet} = \sigma T_m^4 \alpha_p F_4 A_v , \quad T_p \neq C \text{ (dark side of planet)} \tag{B-47a}$$

$$\frac{q_{planet}}{A_v} = \sigma T_m^4 \alpha_p F_4 , \quad T_p \neq C \text{ (dark side of planet)} \tag{B-47b}$$

where F_4 is found by table look-up (see Eq. (B-46b)). The incident heat rate is

$$\frac{q_{planet}}{A_v} = \sigma T_m^4 F_4 , \quad T_p \neq C \text{ (dark side of planet)} \tag{B-47c}$$

6. <u>Albedo heat flux, oriented vehicle</u>: The solar heat reflected from dA_p and absorbed by A_v , shown in Fig. B-6, is

$$dq_{albedo} = \frac{E \cos \phi_p \cos \phi_v dA_p \alpha_s \epsilon_s A_v}{\pi \rho^2} \tag{B-48}$$

Substituting the planet element's effective emissive power given in Eq. (B-35), letting $\epsilon_s = 1$, simplifying, and integrating gives

$$q_{albedo} = SR\alpha_s A_v \iint \frac{\cos\beta \cos\phi_p \cos\phi_v}{\pi\rho^2} \, dA_p \tag{B-49}$$

The above definite integral is expressed in Eq. (B-41). The desired relations are found by combining Eq. (B-41) and Eq. (B-49).

$$q_{albedo} = SR\alpha_s F_3 A_v \tag{B-50a}$$

$$\frac{q_{albedo}}{A_v} = SR\alpha_s F_3 \tag{B-50b}$$

where F_3 is found by table look-up (see Eq. (B-41)). The impinging albedo is

$$\frac{q_{albedo}}{A_v} = SR\ F_3 \tag{B-50c}$$

APPENDIX C

DISCUSSION OF PRACTICAL INTEGRATION STEP-SIZE

The only feasible method to increment time in the numerical integration of the governing temperature equation is to increment the true anomaly and compute the corresponding change in time (see p. 32). This procedure is expressed mathematically as

$$\phi_{n+1} = \phi_n + \Delta\phi \tag{C-1}$$

and

$$\Delta t_{n+1} = t(\phi_{n+1}) - t(\phi_n) \tag{C-2}$$

where $\Delta\phi$ is a constant.

Since the analysis is applicable to all planetary orbits, the magnitude of Δt_{n+1} depends not only on $\Delta\phi$, but also upon variables such as orbit eccentricity and semimajor axis, vehicle position in orbit, and the planet being orbited. This dependence is illustrated by comparing times corresponding to a fixed true anomaly for three earth satellites. For $\Delta\phi = 1°$, Δt is 0.3 min. for the Explorer which was put into a low circular orbit, 4.0 min. for Syncom which is in a large circular orbit, and varies from about 0.3 to 10.0 min. for EGO which is in a large, eccentric orbit. These widely varying times are one reason why it is necessary to refer to the length of the integration interval in terms of practicality rather than as a fixed $\Delta\phi$.

There are three conditions that can make the integration interval impractical. Two of these are controlled by the program. The conditions and their control are described below:

1. Δt_{n+1} can be so large that the one-step truncation error temporarily influences the accuracy of the integration.

To minimize computation time the interval should be large as d^2T/dt^2 approaches zero, and to insure an accurate solution the interval should be small as d^2T/dt^2 becomes large. This philosophy is expressed mathematically as

$$\Delta t_1' \propto \frac{1}{\frac{d^2T_n}{dt_n^2}} \qquad \text{(C-3)}$$

The increment, $\Delta t_1'$, is calculated from this equation.

2. Δt_{n+1} can be so large that the equilibrium temperature is reached and vastly exceeded within one interval thus causing the solution to be unstable.

This condition occurs if $dT/dt \gg 1$ which could be caused by the vehicle skin having negligible heat capacity ($\rho C_p h \rightarrow 0$) or by an unrealistic initial temperature, T_o . The time increment, $\Delta t_2'$, required to reach equilibrium temperature in one interval is calculated.

The intervals $\Delta t_1'$, $\Delta t_2'$, and Δt_{n+1} are compared and the smallest value is selected and used to numerically integrate the appropriate temperature equation. If the program subdivides the time increment Δt_{n+1} into two or more values, $\Delta t'$, the entire procedure is repeated in steps until $\sum \Delta t' = \Delta t_{n+1}$.

A third impractical interval exists if $\Delta\phi$ is so large that the assumption of constant heat fluxes within the interval is absurd. The program will not use time increments that are larger than those computed from the value of $\Delta\phi$ in the input data; therefore, the program user must exercise some judgment in choosing $\Delta\phi$ so that it is small enough to be meaningful but large enough to allow fast computation speed.

MRI has found from its experience that $\Delta\phi = 10°$ is a reasonable value to use in the input data. Significantly smaller values have increased the running speed noticeably while larger values have produced inaccuracies in the results due to the "constant heat flux" assumption being absurd.

N64-27901

ERRATA SHEET

for

Final Report: "Orbiting Satellite Surface Temperature Prediction and Analysis," by Finch et al.

1. Change 8 to 4 in the following expressions: Eqs. (17b) and (18b); p. 26; Eq. (B-16c), p. 56; Eq. (B-30c), p. 60; Eq. (B-33c), p. 62; and Eq. (B-38c), p. 63.

2. Change 16 to 8 in the following expressions: Eq. (19), p. 26 and Eq. (B-31), p. 60.

3. Change 4 to 2 in Eq. (B-23), p. 57.

4. Change Eq. (B-22), p. 57 to:

$$\iint \frac{\cos \phi_p}{\rho^2} \cdot dA_p = 2\pi \left\{ 1 - \left[1 - \left(\frac{r_p}{D} \right)^2 \right]^{\frac{1}{2}} \right\}$$